

**Hadley Centre**

*for Climate Predictions and Research*



**Effects of changing physical parametrisations  
on the simulation of the Asian summer monsoon  
in the UK Meteorological Office Unified Model**

by:

G. M. Martin and M. K. Soman

Hadley Centre, Meteorological Office Bracknell, UK  
Indian Institute of Tropical Meteorology, Pune, India

**HCTN 17**

*Hadley Centre Technical Note*

**September 2000**



**The Met.Office**

# Effects of changing physical parametrisations on the simulation of the Asian summer monsoon in the UK Meteorological Office Unified Model

G.M. Martin<sup>1</sup> and M.K. Soman<sup>2</sup>

<sup>1</sup>Hadley Centre, Meteorological Office, Bracknell, UK

<sup>2</sup>Indian Institute of Tropical Meteorology, Pune, India

16<sup>th</sup> July 1999

Correspondence to:

Dr G.M. Martin,

Hadley Centre for Climate Prediction and Research, Meteorological Office,

London Road, Bracknell, Berks., RG12 2SY, UK

E-mail: gmmartin@meto.gov.uk

Tel: +44 (0)1344 856893

# Abstract

The Asian summer monsoon is an important component of the atmospheric circulation. In order for the countries under its influence to benefit from seasonal predictions of monsoon rainfall, it is essential that GCMs are able to produce a reasonable simulation of both the mean monsoon circulation and rainfall distribution, and its intraseasonal and interannual variability. The influence of four major changes in model physics on the simulation of the Asian summer monsoon in the UK Meteorological Office's Unified Model is investigated by comparing two recent climate versions. The new version, HadAM3, includes changes to the radiation, surface, convection and boundary layer schemes. The overactivity of the monsoon is increased in this model version, and whilst there are some improvements in the precipitation distribution there are also some detrimental effects. There are some changes to the mean monsoon seasonal cycle, with a slightly later monsoon retreat in HadAM3 than in HadAM2b, whilst the timing of the monsoon onset is improved in HadAM3. Very little difference is made to the representation of interannual variability of the monsoon circulation, but that of precipitation is improved slightly. The characteristics of the dominant mode of intraseasonal variability are similar in the two runs, but this mode is rather more active in HadAM3 than in HadAM2b, and its timescale is in better agreement with observations.

Investigation of the influence of individual changes in model physics on the mean monsoon simulation suggests that the change to the radiation scheme results in a slight overall intensification of the monsoon, but that there is also a redistribution of the precipitation. Small changes in the pattern of the dominant modes of intraseasonal variability between HadAM3 and HadAM2b can also be attributed to inclusion of this scheme. Changes to the surface exchange scheme have no significant effect on the mean monsoon simulation, but they do improve the timescales of the intraseasonal variability. The inclusion of convective momentum transports (CMT) weakens the flow at upper levels, but the monsoon circulation at lower levels is strengthened. Many of the changes in the precipitation distribution between HadAM3 and HadAM2b, along with the improvement in the timescale of intraseasonal variability, may also be attributed to the inclusion of CMT. The effects of changes to the boundary layer mixing scheme appear to be similar to those of including CMT. This behaviour is thought to arise due to unrealistic interactions between the boundary layer and convection schemes in the Unified Model.

# 1. Introduction

The simulation of the Asian Summer Monsoon (ASM) and its variability remains a significant challenge for general circulation models (GCMs). The ASM is a major component of the atmospheric circulation, and the economies and livelihood of the populations of India and south-east Asia depend heavily on the rainfall associated with it. In order for these countries to benefit from seasonal predictions of monsoon rainfall, it is essential that GCMs are able to produce a reasonable simulation of both the mean monsoon circulation and rainfall distribution, and its intraseasonal and interannual variability. In addition, such GCMs are used both to simulate the present climate and to predict future global and regional climate change, so it is essential that the main features of the general circulation are simulated with reasonable accuracy.

Several studies have shown a sensitivity of simulations of the ASM to changes in model resolution (e.g. Sperber et al. 1994; Lal et al. 1997; Stephenson et al. 1998), and physical parametrisations (e.g. Fennessey et al. 1994; Laval et al. 1996; Sperber and Palmer 1996; Ferranti et al. 1999). However, the sensitivity to either of these is not straightforward. The benefits of increasing horizontal resolution may depend on the quality of the monsoon simulation at the original resolution, as well as on the physical schemes themselves. For example, Sperber and Palmer (1996) showed that the relative performance of models with different convective closures depended on their horizontal resolution. It is unlikely that increasing the resolution will compensate for errors in the monsoon simulation which arise due to problems with the representation of physical processes. Similarly, improvements in certain physical parametrisations will inevitably lead to changes in their interaction with the other parametrisations, and this will not necessarily lead to an overall improvement in the simulation.

The quality of the simulation of the ASM in a Hadley Centre climate version (HadAM2b; Stratton 1999) of the Meteorological Office's Unified Model, and the impact upon this of increasing the horizontal resolution, were investigated by Martin (1999). HadAM2b has been used extensively in international collaborative modelling studies, e.g. the Atmospheric Model Intercomparison Project (AMIP; Gates 1992), High REsolution Ten Year Climate Simulations (HIRETYCS; see Stratton 1999), and the World Climate Research Programme/CLimate VARiability (WCRP/CLIVAR) Asian-Australian monsoon intercomparison, where the model is being run by the Indian Institute of Tropical Meteorology (IITM). The IITM is also using HadAM2b

for experimental seasonal predictions of the monsoon, which are considered by the Indian Meteorological Department in their long-range monsoon forecasts.

Martin (1999) showed that HadAM2b produces a reasonable simulation of the ASM, although the monsoon strength, in terms of both circulation and precipitation, is rather overestimated, and the onset is slightly early in comparison with observations. The interannual variability of the monsoon circulation is represented by the model, although the corresponding changes in precipitation are not. In contrast, the dominant pattern of intraseasonal variability in the simulated monsoon appears to represent the active/break cycles, which is in good agreement with observations. Martin (1999) showed that although increasing the model horizontal resolution provides extra detail in the precipitation distribution, the mean monsoon simulation is scarcely altered, and the systematic errors remain.

We now investigate the influence of four major changes in model physics on the monsoon simulation, by comparing the simulation of the ASM in HadAM2b with that from a later climate version, HadAM3. This version of the UM is being used in the second AMIP, and represents a significant improvement over previous versions submitted to AMIP. HadAM3 is also being used in a series of coupled ocean/atmosphere climate simulations, HadCM3 (Gordon et al., 1999), to provide climate predictions for the Intergovernmental Panel on Climate Change (IPCC) 2000 report, as well as for seasonal predictions and investigations of the mechanisms of atmospheric processes. The later model version incorporates changes to the radiation, surface, convection and boundary layer schemes. The first two of these changes involve entirely new schemes, whilst a new parametrisation (of the transport of momentum by convection) has been added to the convection scheme. Each of these new schemes has been documented in the scientific literature and is available for use by the modelling community. The impact of each of these major physics changes on the overall global climate has been investigated by Pope et al. (1999), and we will concentrate here mainly on their impact on the monsoon simulation.

Two ten-year runs, forced by the same sea surface temperatures, are used (the run of version HadAM2b is the one at climate resolution described by Martin, 1999). In addition, six-member ensembles of HadAM2b and HadAM3 (using slightly different sea surface temperatures for each model version) are used to provide estimates of the internal variability of the two models (see Section 4.3). The effects of the changes in model physics on the mean monsoon simulation

are examined using ten year monthly averages of precipitation and horizontal wind components at 850 hPa and 200 hPa. The impact upon interannual and intraseasonal variability of the monsoon in the model is then assessed, using monthly averages of precipitation and zonal wind, and daily means of precipitation and 850 hPa relative vorticity.

## 2. Model Description

The UKMO Unified Model (Cullen 1993) is a gridpoint atmospheric GCM with conservative split-explicit integration scheme (Cullen and Davies 1991), which may be configured for numerical weather prediction or climate modelling. Version HadAM2b (Stratton 1999) is an improved version of the atmosphere component of the coupled ocean-atmosphere climate model HadCM2, described by Johns et al. (1997). Similarly, HadAM3 (Pope et al. 1999) is the atmosphere component of the coupled ocean-atmosphere climate model HadCM3 (Gordon et al. 1999). The main differences in physics between these versions are:

- (i) Edwards-Slingo radiation scheme: a general two-stream scheme in both the shortwave and the longwave (Edwards and Slingo, 1996). This replaces the scheme described by Slingo (1989) and Slingo and Wilderspin (1986) which was used in HadAM2b.
- (ii) MOSES (Met Office Surface Exchange Scheme), which includes coupled soil hydrology and thermodynamics (four-layer model) and an interactive canopy resistance model (Cox et al., 1999). This replaces the scheme described by Lean and Rowntree (1997), used in HadAM2b.
- (iii) Convective momentum transport (Gregory et al., 1997),
- (iv) Removing the representation of non-local mixing of thermodynamic quantities (rapidly-mixing term; Smith 1993) from the boundary layer scheme.

The first three of these are new schemes which introduce more detailed and accurate representations of the physics to which they refer. The change to the boundary layer mixing was made in order to avoid problems with the transport and sink of aerosols (which were included for use in the new radiation scheme), and because of unfavourable interactions with the momentum mixing in the boundary layer. Details of the other (minor) changes made in this climate version can be found in Pope et al. (1999).

### 3. Experimental setup

A ten-year run of HadAM2b, at standard climate resolution of 2.5 deg latitude by 3.75 deg longitude, is compared with a similar run of HadAM3. Both runs are forced by analysed sea surface temperatures (SSTs) and sea ice data for 1979 to 1988. These were prepared, using available in-situ, climatological, and satellite data, for AMIP by the Climate Analysis Center of the National Oceanic and Atmospheric Administration in cooperation with the Center for Ocean-Land-Atmosphere Interactions at the University of Maryland. The data were supplied on a  $2^\circ \times 2^\circ$  grid, and were interpolated onto the model grid. The runs started from the beginning of December 1978 and continued for 10 years and one month. The first month of each run was treated as spinup and not included in the ten year means.

Comparisons are made with the ECMWF Re-Analysis (ERA) fields (ECMWF Reanalysis Workshop, 1996) and the National Oceanic and Atmospheric Administration (NOAA) Climate Prediction Center (CPC) Merged Analysis of Precipitation (CMAP/O) produced by Xie and Arkin (1997). The ECMWF reanalysis project involved reanalysis of the period 1979 to 1994 using the available observations for the period. The dataset formed in this way uses the same model throughout the period, rather than using analyses from a model and assimilation scheme which have evolved with time. Temperature, winds, relative humidity, heights and eddy diagnostics are available on pressure levels. The CMAP/O precipitation dataset is derived from satellite observations of infrared emission and microwave scattering and emission, combined with rain gauge data, allowing a monthly analysis of global precipitation from 1979 to 1997 to be derived.

## 4. Comparison of monsoon simulation in HadAM3 and HadAM2b

### *4.1 Mean monsoon simulation*

Figure 1(a and b) shows wind fields at 850 hPa and 200 hPa, averaged between May and September (MJJAS), and over the ten years of the AMIP run (1979-1988) of HadAM3. The differences between these and similar fields from HadAM2b (which were presented in Martin, 1999) are shown in Figure 1(c and d). It is apparent that in the new version of the model the monsoon circulation is even stronger than in the previous version, and is further from the climatology (shown in Figure 1(e and f)). However, the position of the monsoon westerly jet (Somali jet) core at 850 hPa as it turns eastwards along the coast of Saudi Arabia is slightly

further north in HadAM3 compared with HadAM2b, and is closer to ERA. The upper level wind field is similar between the two model versions, although the easterly jet is slightly stronger in HadAM3, and there is also a noticeable deceleration of the flow over East Africa.

Figure 2 shows the ten year mean MJJAS precipitation distributions for HadAM3 and CMAP/O averaged over the same period, and the difference between the two model versions. In HadAM3, the rainfall in western India is localised in the northwest of the peninsula, and there is less rainfall over the southwest Indian peninsula. Such localisation is not present in the observations. Monthly averages of precipitation (not shown) reveal that the precipitation becomes localised to the north of Bombay by June in HadAM3, whereas in HadAM2b it does not move this far north until July, and is also less localised. There is also excessive rainfall over central northern India in HadAM3, which is not seen in either HadAM2b or the observations. However, HadAM3 does appear to have a better precipitation distribution over the Philippines and over Indonesia compared with HadAM2b, and the rain shadow region over the southeast Indian peninsula is also much better represented. The location of the precipitation maximum over the equatorial Indian Ocean is slightly further northeast in HadAM3 than in HadAM2b, bringing it closer to the observations, but a significant error in its location still remains.

Figure 3 shows the 10 year mean annual cycle of monthly-mean precipitation, averaged over the Indian region (5-30N 70-85E), the Bay of Bengal (10-30N 85-100E) and the East Asian region (5-30N 100-115E), for the model runs compared with the observations. Although the timing of the monsoon seasonal cycle is simulated reasonably well by the model, both versions overestimate its amplitude in the Indian region and over the Bay of Bengal. It is interesting to note that the seasonal cycle of precipitation over the Indian region is similar in the two model runs, even though the precipitation distributions in this region are quite different. Over the Bay of Bengal, there is increased rainfall in the latter part of the season in HadAM3 compared with both HadAM2b and CMAP/O. Analysis of daily rainfall in the three regions indicates that the monsoon retreat is later in HadAM3 than in HadAM2b, with daily rainfall averages for the Indian region and the Bay of Bengal remaining at the high values associated with the established phase until after mid-September, rather than starting to decrease towards the end of August as in HadAM2b. Over the East Asian region, the average precipitation is underestimated by HadAM2b, whereas it is much improved throughout the season in HadAM3.



#### 4.2 *Effects on the monsoon onset*

The primary indicator for the onset of the ASM over India is a sharp and sustained increase in rainfall at raingauge stations in south Kerala (Ananthakrishnan and Soman 1988; Soman and Kumar 1993). For the period 1979-1988, the values given in Soman and Kumar (1993, their Table 2) give a mean date of 3rd June with a standard deviation of 6.6 days. Similar analysis of daily rainfall over south Kerala and the surrounding sea areas (7.75-10.25N 74.875-78.625E) in HadAM2b (Martin 1999) showed that the mean onset date for the ten-year AMIP period was 24th May, with a standard deviation of 13.5 days. The results from HadAM3 show a similar mean onset date (21st May) but a much smaller standard deviation (7.3 days). Although the model runs are relatively short, significance tests show that the difference in the mean onset date between both of the model runs and the observations is significant at the 1% level. However, whilst the standard deviation of the onset date for HadAM2b is also significantly different from the observations, this is not the case for HadAM3. Thus, although the new model version shows a similar tendency for a slightly advanced onset as was seen in HadAM2b, the variability of the onset date is in better agreement with observations.

Comparisons of the monsoon onset in other parts of the region can be made using an objective method proposed by P. Tschuck (Annamalai et al. 1998a). With this method, onset at a particular location is defined as the first day on which the daily mean rainfall exceeds a local threshold (the long-term July average for that location), provided that the average rainfall over the next five days also exceeds that threshold. In addition, the 850 hPa wind direction is required to be within 45 degrees of the long-term July average direction and the speed exceeding  $1 \text{ ms}^{-1}$ . Annamalai et al. (1998a) showed the results of this analysis for ERA precipitation and winds from 1979 to 1993. These are reproduced in Figure 4, along with the mean onset dates for the two model runs. In ERA (Fig. 4(c)), the onset date for Kerala is similar to that given by Soman and Kumar (1993), and the monsoon can be seen to take about 40 days to progress from the southern tip of India to the Gujarat region in the northwest of the peninsula (20-25N, 69-74E). The onset is earliest (about 10th May) over South China, and later (19th June) over the Philippines.

The basic pattern of onset dates is represented well by both model versions, although the tendency for early onset can be seen throughout the region. By these criteria, the onset

over southern India is even earlier in HadAM3, but the rate of northward progression is similar, whereas in HadAM2b the onset over southern India is in better agreement with ERA but the northward progression is faster. Over East Asia and the Philippines, the onset in HadAM3 is slightly later than in HadAM2b, but both are slightly earlier than in ERA. Statistical tests indicate that the differences in onset date between both models and ERA over northeast India and East Asia are significant (at the 1% level), whilst the differences from ERA over southern India are only significant in HadAM3.

Calculation of the standard deviation of the onset dates from ERA (not shown) reveals smaller interannual variability of the monsoon onset date over the Indian peninsula and over East Asia, compared with northern India (in the region of the monsoon trough) and the Philippines. A similar pattern is seen in HadAM2b, although the standard deviations are significantly (at the 1% level) larger in magnitude than ERA over parts of India, the South China Sea, and the East China Sea but significantly smaller over northwest India and China. The standard deviations of onset date in HadAM3 are even larger than HadAM2b over the South China Sea and East China sea, but are significantly smaller than both HadAM2b and ERA over northern and peninsular India.

#### *4.3 Interannual variability*

Model runs which only cover a ten year period are too short to enable either the ability of the model to represent the interannual variability of the monsoon or the impact of changes in physical parametrisations on this aspect of the simulation to be assessed with confidence. Longer runs, or ensembles of runs covering the same period but using different initial conditions, are required. Six-member ensembles of both HadAM2b and HadAM3 are available. However, the analysed SSTs used to force each of these ensembles (the Hadley Centre Global sea-Ice and Sea Surface Temperature (GISST1.1) dataset (Parker et al. 1995) were interpolated in slightly different ways prior to application in the two ensembles, leading to slight differences in the annual cycle and interannual variability of the SSTs. In addition, the GISST1.1 SSTs differ from those used in the AMIP simulations by as much as 1K in several regions, which could lead to small differences in the interannual variability. However, since the model physics is the same in the AMIP and GISST runs for each model version, estimates of the internal variability of each model version can be obtained from the ensembles of runs forced with GISST1.1, thus making comparison of

the interannual variability between the two runs possible.

Figure 5 compares the Webster-Yang monsoon indices (Webster and Yang, 1992) for May to September from each of the model runs with the ECMWF reanalyses. This is a dynamical index for monsoon intensity based on the anomalous vertical shear between 850 hPa and 200 hPa for the region 0-20N 40-110E. The internal variability of each model version has been estimated (following Rowell et al. 1995) by averaging, over the ten year period, the variances of the deviations of the indices for the appropriate GISST ensemble from the ensemble mean. The bars on the results for each model run indicate  $\pm 2$  standard deviations, as calculated from this variance. Both model versions show some skill in reproducing the sign of the interannual anomalies in dynamical monsoon intensity which are seen in ERA, and, in general, where the sign of the index in HadAM2b is incorrect, it is also incorrect in HadAM3 (the exception being 1986). There is no evidence that the changes in physical parametrisations between HadAM2b and HadAM3 have substantially altered the interannual variability of the monsoon circulation in the model.

Figure 6 compares the seasonal mean (MJJAS) precipitation anomalies, averaged over different parts of the monsoon region, between the model runs and the CMAP/O data. It is apparent that the changes in model physics between HadAM2b and HadAM3 have reduced the internal variability of the model's simulation of precipitation in Bay of Bengal region, although the values are similar in the other two regions. The new model version also shows slightly better agreement with the CMAP/O observations. Significance tests show that the amplitude of interannual variability of precipitation in HadAM2b is significantly greater (at the 1% level) than that of the observations in the Bay of Bengal region, but not significantly different in the other two regions. Similar analysis for HadAM3 shows a significantly smaller (at the 5% level) amplitude of interannual variability of precipitation in the Bay of Bengal region than the observations, but no significant difference in the other regions. This suggests only a small improvement in the skill of the model in representing the interannual variability of precipitation in moving from HadAM2b to HadAM3.

Comparisons made by Martin (1999) of the change in horizontal winds and precipitation between El Nino years (1982, 1983 and 1987) and La Nina years (1985 and 1988) in HadAM2b and the observations revealed substantial differences, particularly over East Asia, the Philippines

and the western Pacific, at both model resolutions. Similar comparisons with HadAM3 show that many of the errors in the anomalous wind flow and precipitation differences in HadAM2b are exacerbated in HadAM3. The precipitation differences (MJJAS) in the equatorial region between El Nino and La Nina years in the model runs and CMAP/O are shown in Fig. 7. The overall response of the convection to the changes in SST is good in both model runs, particularly over the Pacific and the Atlantic. However, although the negative anomalies over Indonesia are captured by the models, both have substantial positive anomalies over the west Pacific to the northeast of the Philippines which are not present in CMAP/O. There are some improvements in the anomalous precipitation field in the Bay of Bengal and over China in HadAM3, even though the anomalous wind flow over China and Japan is still incorrect. There are also some improvements in the anomalies over the Indian Ocean in HadAM3. However, this model version also shows decreases in rainfall over western India, and increases over the Indian Ocean to the southwest of the Indian peninsula, between El Nino years and La Nina years, which are not seen in CMAP/O. Similar analysis of the ensembles of runs using each model version but forced by the GISST1.1 SSTs shows many of the same features, suggesting that the differences between the two models, and between the models and the observations, are significant.

Martin (1999) also showed that there was a difference in the timing of the monsoon season in HadAM2b in El Nino years compared with La Nina years, which was also seen in the observations, but to a lesser degree. However, in HadAM3, there is little difference in the timing of the monsoon season between El Nino and La Nina years in any of the three regions, although there is a consistent reduction in precipitation over the East Asian region in the La Nina years, which is the opposite of the change seen in the observations. Similar analysis of the GISST ensembles of the two model versions show the same tendencies, which suggests that these changes are robust. Thus, it appears that the changes in model physics between versions HadAM2b and HadAM3 of the Unified Model alter the response of the timing of the monsoon season to El Nino and La Nina.

#### *4.4 Intraseasonal variability*

The Asian Summer Monsoon exhibits variability within any one season on a variety of temporal and spatial scales. In the Indian region, the intraseasonal variability is dominated by active/break cycles, with periods between 30-60 days. These are thought to be associated with

north-south movement of the Tropical Convergence Zone (TCZ) between two favourable locations, one over southeast Asia and the Indian subcontinent, and the other over the equatorial Indian Ocean (Sikka and Gadgil, 1980). The changes in rainfall over India between active and break periods are considerable and may have a significant effect on the monthly or seasonal mean rainfall. Variability on a shorter timescale of 10-20 days is also observed, which is associated with the life-cycle of synoptic scale systems such as monsoon depressions moving westwards across northern India (Krishnamurti and Bhalme 1976). These tend to occur more frequently during the active phase of monsoon, when the TCZ is over the monsoon trough region, although the monsoon may also revive from a break situation with the formation of a monsoon depression over the head of the Bay of Bengal. This can occur before the next phase of the northward movement of the TCZ.

Intraseasonal variability of the Asian monsoon in the two versions of the Unified Model is examined using daily averages of precipitation and 850 hPa relative vorticity from May to September. The different modes of variability can be separated by calculating the empirical orthogonal functions (EOFs) associated with the time variations of the anomalous precipitation and relative vorticity fields. De-trended daily anomalies are formed by subtracting the smoothed ten-year mean daily seasonal cycle from each year, and frequencies with periods shorter than 8 days are filtered out using a low-pass filter. Since these runs are both relatively short, the results are checked for robustness by dividing the timeseries into two parts and performing the calculations on each half as well as on the whole dataset. Very similar results are found in all three cases for both runs.

Figure 8(a and b) compares the first EOFs of precipitation in the two model runs. This mode describes 10% and 11% of the variance in each case, respectively, and is the dominant mode since it explains nearly twice as much of the variance as the next EOF. Two bands of large variability, one extending from the Western Ghats into south-east Asia, between about 5N-25N, and the other across the Indian Ocean between 5S-15S, are seen in both runs. This is characteristic of the active/break phases of the monsoon (Sikka and Gadgil, 1980). The characteristics of this mode of variability are similar in the two runs, although the “continental” mode is slightly weaker over the Indian region and slightly stronger over East Asia and the Philippines in HadAM3. Similar analyses of 850 hPa relative vorticity (not shown) also show

good agreement between the two model versions, and also compare well with those from the ECMWF and NCAR/NCEP (National Center for Atmospheric Research/National Centers for Environmental Prediction) reanalyses, presented by Annamalai et al. (1998b; their Figure 13), and explain a similar percentage of the variance.

Figure 8(c and d) shows the second EOF of precipitation for each run, describing 6% and 5% of the variance, respectively. In HadAM2b, this mode exhibits an east-west structure indicating oscillations between the Indian region and East Asia. In HadAM3, this mode is more complex, with increases in precipitation in the Indian region and the Bay of Bengal being associated with increases in precipitation over the southern parts of the South China Sea and the Philippines and decreases over the northern parts of these regions. Evidence of an east-west mode of variability in a pattern similar to that shown for HadAM3 was seen in the third EOF obtained from the 40-year NCEP/NCAR reanalyses (Sperber et al. 1998), whilst the second EOF from the reanalyses, in conjunction with the first EOF, described the northward propagation of the active/break cycle (the second and third modes describe similar percentages of the variance). However, the timescale of this mode of variability is shorter in the reanalyses than in either of the model runs.

Figure 9 shows the probability density function (PDF) of PC1 for each of the model runs. If the transition time between active and break phases of the monsoon is shorter than the residence time in either phase, the PDF should be bimodal. Neither model version exhibits such bimodality when all of the ten years are used. However, if only years where the standard deviation of PC1 is greater than 1 are used, some evidence of bimodality can be seen in HadAM3 (Fig. 9, dotted line). None of the years of the HadAM2b run fit this criterion, indicating that this mode of variability is less active in this model version. The latter is also illustrated by the fact that the PDF for HadAM3 is slightly broader than that for HadAM2b. Interestingly, the PDF for the years when this mode is more active in HadAM3 (1980,1983,1986,1988) is biased towards break periods. However, Fig. 9 also shows increases in the strength of the active periods in these years which compensate for this bias. Reference to Fig. 6 shows that in fact none of these years was a weak monsoon year in terms of the seasonal mean precipitation.

Spectral analysis of the two PC1 timeseries shows that whilst in HadAM3 the dominant mode of intraseasonal variability has two distinct timescales of 15-20 days and 35-50 days,

HadAM2b only shows a single timescale of 18-25 days. The existence of variability on the timescale of monsoon depressions in PC1 is to be expected, given the tendency of such systems to be prevalent during the active phase of the monsoon. These results suggest that although the lifecycle of monsoon depressions is quite realistic in the two models, the active/break phases of the monsoon in HadAM3 are more coherent than in HadAM2b, and have a timescale which is in reasonable agreement with that which is observed.

These results illustrated that whilst the patterns of intraseasonal variability in the two model versions are quite similar, the nature of this variability is rather different. Although the sample of data from each of the different models is relatively small, there are indications that the representation of intraseasonal variability has been improved by the changes in physical parametrisations between HadAM2b and HadAM3.

## 5. Effects of individual physics changes

In the previous section it was shown that the new version of the climate model, HadAM3, exhibits both a different mean monsoon simulation and slight differences in interannual and intraseasonal variability. In order to investigate how each of the major changes to the model physics has contributed to these differences, ten year AMIP-style runs, with and without each of these changes, are now compared. It should be noted that the impact of a change in any physical scheme may depend on the state of the other physical schemes present in the model, so that the combined effect of two alterations may be substantially different from the individual effects of either of the changes. In addition, it is difficult to assess the impact on the interannual variability of the simulated monsoon using these relatively short runs. This preliminary investigation therefore concentrates on assessing the overall impact of each of the main physics changes (Edwards-Slingo radiation scheme, MOSES, convective momentum transports and changes to the boundary layer scheme) on the mean monsoon simulation and its intraseasonal variability in HadAM3.

### *5.1 Edwards-Slingo radiation scheme*

The new radiation code is based on two-stream equations in both the shortwave and longwave regions of the spectrum. This means that processes which are important in both spectral regions, such as the overlapping of partially cloudy layers, are treated consistently. The radiative

properties of ice and water are dealt with separately, which allows the impact of different ice habits to be parametrised. In addition, the representation of absorption by gaseous constituents of the atmosphere (particularly water vapour) has been improved.

Pope et al. (1999) showed that the change in radiation scheme is associated with a net warming in the troposphere. This is a result both of reductions in longwave cooling in the lower troposphere (arising mainly from the use of the CKD continuum model (Clough et al. 1989) instead of the RSB model (Roberts et al. 1976)) and increases in shortwave heating throughout most of the troposphere (due to changes in the clear-sky fluxes). Globally, the sensible and latent heat fluxes from the surface are reduced in order to balance the reduction in radiative cooling of the atmosphere. Over the sea, the air-sea temperature difference is reduced, decreasing the convective instability. However, over land, low level moisture is increased considerably through additional moisture convergence resulting from the reduced precipitation over the sea. Thus, precipitation is increased over land (particularly in the tropics) and decreased over the oceans.

Figure 10(a and b) shows the differences in the ten-year MJJAS mean horizontal winds at 850 hPa and 200 hPa resulting from the change in radiation scheme alone. The new radiation scheme is associated with strengthening the monsoon circulation at both upper and lower levels. This may be a result of the increase in the land-sea temperature contrast associated with the warmer land surface temperatures. There is also some contribution, by the change in radiation scheme, to the deceleration of the flow over East Africa which was shown in Figure 1. Figure 10(c) shows the change in the ten-year average precipitation field for MJJAS. As indicated above, inclusion of the new radiation scheme tends to reduce the precipitation over the oceanic areas, particularly the equatorial Indian Ocean, the Arabian Sea, the Bay of Bengal and in the rain shadow region of southeast India, whilst increasing the rainfall over central northern India, along the southern slopes of the Himalayas, and over East Asia. However, there are also increases in precipitation over the Philippines and the western Pacific. This may be a result of the increased monsoon circulation. Timeseries of monthly mean precipitation, averaged over three parts of the monsoon region (not shown) show that these changes persist throughout the monsoon season.

The impact on the monsoon onset of including the new radiation scheme (using the objective method described above) is in slightly delaying the onset over the Philippines, which is in the same sense as the change between HadAM2b and HadAM3, but also in accelerating the



northward progression of onset from southern India to Gujarat, which is in the opposite sense, indicating that it must be counteracted by one of the other physics changes.

Comparison of EOFs of precipitation from the run without the Edwards-Slingo radiation scheme (Fig. 11) with those from HadAM3 and HadAM2b (Fig. 8) suggests that the increase in the strength of the first EOF pattern in East Asia and the Philippines, and the changes in the characteristics of the second EOF between HadAM3 and HadAM2b, are associated with the inclusion of the new radiation scheme. In addition, spectral analysis of the timeseries of PC1 in the run with the old radiation scheme suggests that the 15-20 day timescale of this dominant mode of variability is strengthened when the Edwards-Slingo radiation scheme is included. This suggests an increase in the frequency of monsoon depressions, which may be a result of the increased moisture convergence associated with the net tropospheric warming described above. The increased average rainfall over central northern India is consistent with such a change.

### *5.2 Met Office Surface Exchange Scheme (MOSES)*

The new land surface scheme, MOSES, incorporates an interactive plant photosynthesis and conductance module, and a new soil thermodynamics scheme which simulates the freezing and melting of soil water and takes account of the dependence of soil thermal characteristics on the frozen and unfrozen components. Climate tests show that soil water freezing tends to warm the high latitude land in the northern hemisphere during autumn and winter, whilst the increased soil water availability (primarily as a result of increased root depths) alleviates a spurious drying in the mid-latitudes in summer. The impact of this scheme on the monsoon simulation is now investigated. It should be noted that several minor changes were made to the model after MOSES was first included, and it is only possible, at present, to compare the monsoon simulation with and without MOSES before these minor changes were made.

Examination of changes in the circulation and precipitation distribution between the runs with and without MOSES shows that the core of the monsoon jet at 850 hPa is slightly further north over the monsoon region, the upper level easterly flow over East Africa is weakened slightly, and precipitation amounts over land tend to be increased at the expense of those over the sea, probably due to the increased soil moisture availability. However, these differences are considerably smaller than those which can be attributed to the other main physics changes. This suggests that the change in land surface scheme between these two model versions has

only a small impact on the mean monsoon simulation. However, including MOSES advances the monsoon onset over the Philippines but delays it over southern India, as well as slowing the northward progression of the monsoon over India (Figure 12). These changes are in the same sense as the changes between HadAM2b and HadAM3. The reduction in the rate of northward progression over India counteracts the effects of the change in radiation scheme on this aspect of the monsoon onset.

Examination of the intraseasonal variability of the monsoon in the runs with and without MOSES suggests that although the patterns of variability described by the first two EOFs of precipitation are similar in both runs, the timescale of the active/break cycles is lengthened from 27-40 days without MOSES to 35-60 days with MOSES, and the 20-25 day timescale is also strengthened. This is similar to the findings of Ferranti et al. (1999), who showed (using the ECMWF model) that including land surface feedbacks enhanced the lower frequencies of monsoon intraseasonal variability, whilst the spatial pattern of variability was unaffected. This suggests that although land surface feedback is allowed in both versions of the surface scheme compared in the present study, these feedbacks may be more realistic with MOSES. Soil moisture availability over Indian land areas (10-24N, 70-90E) is about 35% higher in the run with MOSES than in the run without, although the surface temperatures are very similar. Analysis of the time evolution of soil moisture availability between July and mid-September shows that the 30-50 day timescale is dominant in both runs, with a 15-20 day timescale also being present in the run with MOSES. The spectral power in the 30-50 day timescale of soil moisture fluctuations with MOSES is slightly larger than in the run without MOSES. However, in some years of each run there is poor correlation between fluctuations in precipitation and soil moisture in this model, indicating that the feedback between the soil hydrology and precipitation in the model is complex. Further work is needed to understand this interaction.

### *5.3 Convective momentum transport (CMT)*

One of the main physical changes incorporated in HadAM3 was a parametrisation for the vertical transport of horizontal momentum by convection. Including this transport is found to have a large positive impact on the momentum budget of the atmosphere, improving the mean circulation especially in the tropics (Gregory et al. 1997, Pope et al. 1999). However, there are also some detrimental effects, such as a strengthening of the Hadley circulation (which is already too

strong), occurring as a response of the model dynamics to the change in the convection scheme. In addition, Inness and Gregory (1997) found that inclusion of CMT in HadAM2b weakened the eastward-propagating tropical intraseasonal (30-60 day) oscillation (the Madden-Julian oscillation, MJO; Madden and Julian 1971) and suppressed the variability of tropical convection on the equator, particularly in the Pacific. Intraseasonal variability in the Asian summer monsoon occurs on a similar timescale, and there is a strong relationship, in some years, between the north-south modulation of the TCZ and the eastward-propagating intraseasonal modes (Annamalai et al. 1998a). Thus, we might expect the inclusion of CMT to have some impact on both the mean monsoon and its intraseasonal variability.

The parametrisation for CMT was included in the early stages of the development of HadAM3. However, a ten-year AMIP-style run with CMT switched off was carried out shortly before the model version HadAM3 was finalised. Figure 13(a and b) shows the changes in 850 hPa and 200 hPa wind fields for MJJAS, averaged over the ten year period, arising due to the inclusion of CMT. At 200 hPa, the easterly flow is decelerated as the vertical transport of horizontal momentum by convection provides a westerly drag at upper levels. Such transport should also decelerate the low level jet at 850 hPa, but although there is some deceleration over the southern Arabian Sea at this level, the flow is accelerated along the central part and northern edge of the jet and across the central Indian peninsula. The monsoon trough is deepened, but the westerly flow over the Philippines is reduced slightly. There is also a broadening of the cross-equatorial flow, although the subtropical easterly jet over the southern Indian Ocean is weakened. At 200 hPa, it appears that the deceleration of the flow over East Africa, shown in Figure 1, is largely associated with the inclusion of CMT.

Figure 13(c) shows the difference in ten-year mean MJJAS precipitation distributions between the runs with and without CMT. This can be compared with the precipitation differences between HadAM3 and HadAM2b, shown in Figure 2(b). It is clear that many of the changes in the precipitation distribution (including the localisation of the rainfall in the northwest of the peninsula, the improvement in the rain shadow region over the southeast Indian peninsula, the increased precipitation over the Bay of Bengal, the northeastward movement of the precipitation over the equatorial Indian Ocean, and the improvement in the precipitation distribution over the Philippines and over Indonesia) are a consequence of including CMT.

Detailed investigations of the effects of CMT on the monsoon simulation have been carried out using ten-member ensembles of 5-day runs, with and without CMT. This approach allows the immediate impacts of CMT to be assessed before any feedbacks through the large scale flow have occurred. The use of an ensemble average smooths out some of the internal variability in the short runs.

The ensemble mean wind increments due to the different physics schemes are averaged over the first day of the runs. At low levels, the wind increments due to the boundary layer scheme are decreased when CMT is included, as the convection scheme takes over some of the momentum mixing. The convection scheme is also now able to transport momentum between the boundary layer and the free troposphere. The CMT accelerates the low-level flow (at 970 hPa) over the west coast of India (Fig. 14b), but the boundary layer scheme more than compensates for this. Thus, the net change in the wind field and its divergence due to the two schemes (BL+CMT, Fig. 14c) is quite different from that due to CMT alone. Figure 14(a and c) shows that, at 970 hPa, the change in the daily mean wind field and its divergence between the ensembles with and without CMT is largely forced by the change in the total BL+CMT wind increments. The remaining changes in the wind field in Fig. 14a, including the net westerly acceleration over northwest India and the changes in the flow over the equatorial Indian Ocean, occur as the large-scale dynamics adjusts to the changes in the BL+CMT increments.

At 970 hPa, the changes are such that there is increased convergence over northwest India and over the northwest of the Bay of Bengal, and increased divergence over central and southwest India. At upper levels, a westerly acceleration occurs over India and the Bay of Bengal as the convection scheme mixes westerly momentum upwards from the lower levels. The changes in the wind field are such that there is increased divergence in this region and a corresponding increased convergence further south (Fig. 14(d and e)).

Figure 14(f) shows the average change in daily precipitation for the first day of the ensembles. The pattern of rainfall changes which was associated with the inclusion of CMT in Fig. 13 can be identified as an immediate impact. Comparison with the changes in the divergence at upper and lower levels suggests that the precipitation changes are forced partly by the changes at low levels, which will affect the triggering of convection, and partly by the changes at upper levels, which will tend to alter the depth of convection, suppressing it over southwest India

whilst deepening it over northwest India. The location of the Gujarat region in northwest India with respect to the Somali jet, combined with its coastal position, makes the region particularly conducive to convection. Thus, a positive feedback is likely from these immediate impacts as, for example, increased triggering of convection in northwest India will enhance the pattern of convergence/divergence anomalies.

These sensitivity tests suggest that the pattern of changes in the mean monsoon simulation in the Indian region when CMT is included is an immediate and local impact of this change, rather than a result of longer-term changes in the large-scale circulation. Further analysis of the ensemble of 5-day runs suggests that the inclusion of CMT also alters the evolution of convective disturbances over the western Pacific. Such systems typically form over the equatorial west Pacific and move northwestwards across the Philippines into southeast Asia. Examination of the movement of individual systems in the runs with and without CMT indicates that this northwestward movement is decelerated when CMT is included. It is not possible to say whether it is this direct change in evolution which is responsible for the alterations in the precipitation distribution seen in Fig. 13, rather than a feedback through changes in the circulation. However, the improved agreement with the observed precipitation distribution in this region (Fig. 2(c)) suggests that the new equilibrium reached by the model when CMT is included is more realistic with respect to the formation and evolution of tropical cyclones in the western Pacific.

Including CMT in HadAM3 results in earlier monsoon onset over India but later onset over East Asia and the Philippines (Figure 15a). There is also a decrease in the interannual variability of the monsoon onset date in the Indian region and an increase over East Asia and the Philippines (Figure 15b). These changes are similar to those between HadAM2b and HadAM3.

The impact of including CMT on the intraseasonal variability of the monsoon is mainly in altering the timescale of variability, rather than its pattern. Spectral analysis of PC1 from the runs with and without CMT shows that the timescale of this mode of variability increases from 18-30 days without CMT to 25-40 days with CMT. This suggests that including CMT improves the timescale of the active/break cycles. However, analysis of the eastward-propagating intraseasonal mode in HadAM3 (using the methods of Slingo et al., 1996) shows that the MJO is much weaker in HadAM3 than in HadAM2b. Similar analysis of the runs with and without CMT shows that the MJO signal is weakened when CMT is added, consistent with the findings

of Inness and Gregory (1997). The apparent mis-match between the existence of a coherent MJO signal and the existence of variability in PC1 on the 30-60 day timescale suggests that the two are not strongly linked in the model. Indeed, Inness and Gregory (1997) also showed that although the variance of outgoing longwave radiation (filtered to isolate variability on a 25-70 day timescale) in their run with CMT was reduced along the equator, the values over the Asian monsoon region were similar to those in HadAM2b, suggesting that much of the variability in this region on this timescale was localised. Comparisons of the variance of filtered precipitation anomalies in the runs with and without CMT give similar indications. Further investigation of these findings may help us to understand the mechanisms by which both of these modes of variability are maintained in the model.

#### *5.4 Changes to boundary layer mixing scheme*

In HadAM2b, two schemes are available for calculating turbulent fluxes at the surface and through the boundary layer: a local mixing scheme, using a mixing coefficient which is a function of a mixing length, the local wind shear and atmospheric stability, and a representation of non-local mixing (rapidly-mixing boundary layer scheme, RMBL) which uniformly distributes the heating and moistening resulting from the divergence of the fluxes between the surface and the top of the boundary layer. The total flux at a given model layer interface within a mixed layer is the sum of the local and non-local fluxes. The rapidly-mixing scheme was included because, in unstable regions, the fluxes are in fact not closely related to the local gradients: the mixing eddies have a large vertical extent. Also, other parts of the model, particularly the convection scheme, can influence the local values of stability and thereby limit the depth over which the boundary layer scheme operates. This is an artifact of the model, which allows both the convection and boundary layer scheme to operate in the boundary layer.

However, the RMBL did not directly address the problems of lack of vertical mixing of momentum by the boundary layer scheme which result from the local mixing scheme (although the changes to the atmospheric stability associated with the RMBL did tend to increase the momentum mixing slightly). Also, during the development of HadAM3, it was found that the RMBL produced unfavourable interactions with the transport and sink of aerosols (which were introduced in HadAM3). Therefore, the RMBL was switched off in HadAM3, along with other minor modifications to the boundary layer scheme. In addition, a fix was applied to the

convection scheme in order to reduce the problems of the convection scheme altering the local stability in the boundary layer. It should be emphasised that these modifications were made in order to address problems which are specific to the Unified Model. However, the following analysis indicates that such modifications affect the way the model responds to the addition of CMT, showing that it is important to take the configuration of the boundary layer scheme into account when examining the sensitivity of the model simulation to changes in the convection scheme in this model.

The impact of switching off the RMBL is assessed by comparing the ten year run of HadAM3 with a similar run in which the RMBL was switched on again and the fix to the convection scheme removed. Figure 16(a and b) shows the change to the ten-year mean MJJAS horizontal wind fields at 850 hPa and 200 hPa between the two runs. At 850 hPa, the changes are relatively small, but comparison with Fig. 13(a) reveals that the pattern of changes is similar in many ways to that which occurs due to the inclusion of CMT. A notable exception is the acceleration of the westerly jet over the northern Arabian Sea, which is not seen in Figure 16(a). At 200 hPa, the most noticeable difference is the deceleration of the flow over East Africa, which was also seen in Fig. 13(b). Figure 16(c) shows the corresponding changes in precipitation. Once again, comparison with Fig. 13(c) reveals strong similarities between the impacts of these two changes.

The impact of removing the RMBL on the intraseasonal variability of the monsoon in HadAM3 is, in a similar manner to that of including CMT, mainly in altering the timescale of variability, rather than its pattern. Spectral analysis of PC1 from the run with the rapidly-mixing boundary layer scheme switched on shows no 30-50 day peak and only a weak signal at 15-20 days. Calculating the monsoon onset dates, using the objective method, for the runs without and with the RMBL shows that switching off RMBL leads to earlier onset over India, but it is also earlier over the Philippines. The interannual variability of the monsoon onset date is decreased over India and increased over East Asia and the Philippines. Many of these changes are, once again, similar to those associated with including CMT.

The fact that changes to the convection and boundary layer schemes appear to have similar effects on the monsoon simulation suggests that turning off the RMBL enhances the effects of CMT. Detailed investigations using short sensitivity tests (similar to those used for CMT in

the previous section) suggest that this is because more of the transport of momentum in the boundary layer is now being done by the convection scheme, even though a fix to the convection scheme has been added to try to limit this. Ideally, the overall momentum mixing should remain the same, regardless of which scheme is responsible for it. The fact that it does not illustrates that the momentum mixing is not matched by the two schemes. The sensitivity of the simulation to the balance of boundary layer mixing between the boundary layer and convection schemes in the Unified Model is an unsatisfactory situation which has been known for some time. It is currently being addressed with the development of a revised formulation for the boundary layer mixing.

## 6. Summary

The UK Meteorological Office Unified Model is used widely by the modelling community for climate predictions as well as for seasonal forecasts and investigations of the mechanisms of atmospheric processes. Documenting both the quality of the UM's simulation of such an important component of the atmospheric circulation as the Asian summer monsoon, and the sensitivity of this simulation to both minor and major changes to the physical parametrisations, provides essential information to all users of the model. In addition, such information helps the scientific community to interpret studies and predictions made using the model within the context of an understanding of the limitations and sensitivities of the model. In order to investigate the influence of changes in model physics on the monsoon simulation, two recent versions of the UM, at climate resolution, have been compared. The new version, HadAM3, includes changes to the radiation, surface, convection and boundary layer schemes.

The results suggest that these changes to the model physics do not reduce the overactivity of the monsoon in the model, but do alter some aspects of the mean circulation and the precipitation distribution. Improvements in the simulation include a better precipitation distribution over the Philippines and over Indonesia, and better representation of the rain shadow region over the southeast Indian peninsula. The location of the precipitation maximum over the equatorial Indian Ocean is also slightly closer to the observations. However, some aspects of the mean monsoon simulation are worse in the new model version, for example, the increased strength of the monsoon circulation, the localisation of precipitation to the north of Bombay, and excessive rainfall over central northern India. There are also some changes to the mean



monsoon seasonal cycle, with a slightly later monsoon retreat in HadAM3 than in HadAM2b. However, although the mean onset date is similar in the two models (and earlier than in the observations), HadAM3 exhibits a significantly smaller standard deviation of onset date over southern India than HadAM2b, which is in better agreement with the observations.

Very little difference is made to the representation of interannual variability of the monsoon circulation, but the representation of the interannual variability of precipitation is improved slightly. The internal variance of the model's simulation of precipitation in the Bay of Bengal region is also reduced in HadAM3. There are some similarities between the responses of the two model versions to the SST changes associated with El Nino and La Nina, although many of the errors in the anomalous wind flow and precipitation patterns in HadAM2b are exacerbated in HadAM3. It is also found that there is no substantial difference in the timing of the monsoon season in El Nino years compared with La Nina years in HadAM3, which is different from HadAM2b.

The characteristics of the dominant mode of intraseasonal variability are similar in the two runs, and this mode explains a similar percentage of the total variance in each case. However, this mode is rather more active in HadAM3 than in HadAM2b, and the PDF of PC1 for HadAM3 does exhibit bimodality, indicating that the transition time between active and break phases of the monsoon is shorter than the residence time in either phase. Also, in HadAM3, the dominant mode of intraseasonal variability exhibits two distinct timescales which are associated with the life-cycle of monsoon depressions moving westwards across northern India and with the north-south movement of the TCZ. This is in reasonable agreement with that which is observed. However, HadAM2b only exhibits the shorter of these two timescales.

In order to investigate the influence of individual changes in model physics on the mean monsoon simulation, runs which were carried out to test the different physics changes implemented in HadAM3 have been analysed. These suggest that the use of the Edwards-Slingo radiation scheme results in a slight overall intensification of the monsoon, but that there is also a redistribution of the precipitation. Both of these changes are related to a net warming of the troposphere which occurs through reductions in longwave cooling and increases in shortwave heating. The small changes in the pattern of the dominant modes of intraseasonal variability between HadAM3 and HadAM2b can also be attributed to inclusion of this scheme. The inclu-

sion of MOSES does not appear to have a significant effect on the mean monsoon simulation, except in altering slightly the position of the monsoon jet over the Arabian Sea and increasing precipitation over land slightly. However, including MOSES does affect the timescale of the dominant mode of intraseasonal variability, lengthening it from 27-40 days to 35-60 days, and strengthening the 20-25 day timescale, possibly as a result of improved land surface feedbacks. Both the inclusion of MOSES and the use of the Edwards-Slingo radiation scheme delay the monsoon onset over the Philippines, but these two schemes have opposite effects on the rate of northward progression of the monsoon over India.

The inclusion of convective momentum transports weakens the flow at upper levels, but at lower levels the model adjusts to the change in the balance of momentum mixing between the convection and boundary layer schemes by strengthening the monsoon circulation. In addition, it is found that many of the changes in both the precipitation distribution and the monsoon onset dates between HadAM3 and HadAM2b may be attributed to the inclusion of CMT. The latter also appears to improve the timescale of the active/break cycles, although it is found to weaken the MJO (in agreement with Inness and Gregory, 1997), suggesting that the existence of a coherent MJO signal and the existence of variability in PC1 on the 30-60 day timescale are not strongly linked in the model. It is possible that the sensitivity of the maintenance of both of these modes of variability in the model to the inclusion of CMT may help us to understand the mechanisms by which they are maintained in the real atmosphere.

This model also shows a sensitivity in its monsoon simulation to modifications made to the boundary layer scheme, which can, in a similar manner to the inclusion of CMT, be attributed to changes in the balance of momentum mixing between the boundary layer and convection schemes in the lower atmosphere. These are artifacts of the current model setup and are undesirable, particularly since they alter the sensitivity of the monsoon simulation to physical improvements in the convection scheme. Care must therefore be taken in assessing the impact of such changes in this model. It is hoped that revisions to the boundary layer and convection schemes in future model versions will eliminate this problem.

This study illustrates the sensitivity of the simulation of the Asian summer monsoon in the Unified Model to changes in some of its physical parametrisations. An important scientific conclusion of this work is that even when such changes are considered to be improvements

to the model, such as a more detailed representation of radiative transfer, or the inclusion of vertical transport of momentum by convection, the result is not necessarily an improved simulation everywhere. The complexity of the Asian monsoon system and its variability, combined with the regional nature of the precipitation distribution and the importance of this to the economies of the countries under its influence, make the accurate simulation of the monsoon an essential but challenging requirement of global climate modelling. Understanding the manner in which changes to the physical parametrisations alter the monsoon simulation should allow improvements to be made in future model versions.

### *Acknowledgements*

The authors would like to thank Dave Rowell and David Sexton for their help with the statistical analyses. We also thank Peter Tschuck for providing the analyses of onset dates from ERA. This work was carried out under the Studies of the Hydrology, Impact and Variability of the Asian summer monsoon (SHIVA) project, funded by European Union contract no. ENV4-CT95-0122, and was begun during M.K. Soman's visit to the Hadley Centre in 1997. The support of the British Council in providing a visiting fellowship is gratefully acknowledged.

## **References**

- Ananthakrishnan R, Soman MK (1988) The onset of the southwest monsoon over Kerala: 1901-1980. *J Climatology* 8:283-296
- Annamalai H, Slingo JM, Hodges K, Rupakumar K, Tschuck P (1998a) SHIVA Atlas: Climatology of the Asian Summer Monsoon from ECMWF Reanalyses and Analyses for the AMIP II period (1979-95). Available from the Centre for Global Atmospheric Modelling, University of Reading, Reading, UK.
- Annamalai H, Slingo JM, Sperber KR, Hodges K (1998b) The mean evolution and variability of the Asian summer monsoon: Comparison of ECMWF and NCEP/NCAR reanalyses. *Mon Weath Rev* (accepted)
- Cox PM, Betts RA, Bunton C, Essery RLH, Rowntree PR, Smith J (1999) The impact of new land surface physics on the GCM simulation of climate and climate sensitivity. *Clim Dyn* (accepted)

- Clough SA, Kneizys FX, Davies RW (1989) Line Shape and the Water Vapour Continuum. *Atmos Res* 23:229-241
- Cullen MJP (1993) The unified forecast/climate model. *Meteorol Mag* 122:81-94
- Cullen MJP, Davies T (1991) A conservative split-explicit integration scheme with fourth-order horizontal advection. *Q J R Meteorol Soc* 117:993-1002
- Edwards J, Slingo A (1996) Studies with a flexible new radiation code. I: Choosing a configuration for a large-scale model. *Q J R Meteorol Soc* 122:689-720
- Fennessey MJ, Kinter JL III, Kirtman B, Marx L, Nigam S, Schneider E, Shukla J, Straus D, Vernekar A, Xue Y, Zhou J (1994) The simulated Indian monsoon: A GCM sensitivity study. *J Clim* 7:33-43
- Ferranti L, Slingo JM, Palmer TN, Hoskins BJ (1999) The effect of land surface feedbacks on the monsoon circulation. *Q J R Meteorol Soc* 125:1527-1550
- Gates LW (1992) AMIP: the Atmospheric Model Intercomparison Project. *Bull Am Meteorol Soc* 73:1962-1970
- Gordon C, Cooper C, Senior C, Banks H, Gregory J, Johns T, Mitchell J, Wood R (1998) The simulation of SST, sea ice extents and ocean heat transports in a coupled model without flux adjustments. *Clim Dyn* (submitted)
- Gregory D, Kershaw R, Inness PM (1997) Parametrization of momentum transport by convection. II: Tests in single-column and general circulation models. *Q J R Meteorol Soc* 123:1153-1183
- Inness PM, Gregory D (1997) Aspects of the intraseasonal oscillation simulated by the Hadley Centre atmospheric model. *Clim Dyn* 13:441-458
- Johns TC, Carnell RE, Crossley JF, Gregory JM, Mitchell JFB, Senior CA, Tett SFB, Wood RA (1997) The Second Hadley Centre Coupled Ocean-Atmosphere GCM: model description, spinup and validation. *Clim Dyn* 13:103-134
- Krishnamurti TN, Bhalme HN (1976) Oscillations of a monsoon system. Part I: Observational aspects. *J Atmos Sci* 33:1937-1954

- Lal M, Cubasch U, Perlwitz J, Waszkewitz J (1997) Simulation of the Indian monsoon climatology in the ECHAM3 climate model: Sensitivity to horizontal resolution. *Int J of Clim* 17:847-858
- Laval KM, Raghava R, Sadourny R, Forichon M (1996) Simulation of the 1987 and 1988 Indian monsoon using the LMD GCM. *J Clim* 9:3357-3371
- Lean J, Rowntree PR (1997) Understanding the sensitivity of a GCM simulation of Amazonian deforestation to the specification of vegetation and soil characteristics. *J Clim* 10:1216-1235
- Madden RA, Julian PR (1971) Detection of 40-50 day oscillation in the zonal wind in the tropical Pacific. *J Atmos Sci* 28:702-708
- Martin GM (1999) The simulation of the Asian Summer Monsoon, and its sensitivity to horizontal resolution, in the UK Meteorological Office Unified Model. *Q J R Meteorol Soc* 125:1499-1525
- Parker DE, Folland CK, Bevan A, Ward NM, Jackson M, Maskell K (1995) Marine surface data for analyses of climatic fluctuations on interannual to century timescales. In: Martinson DG, Bryan K, Ghil M, Hall MM, Karl TR, Sarachik ES, Sorooshian S, Talley LD (eds) *Natural Climate Variability on Decade to Century Time scales*. National Academy Press, Washington pp241-250
- Pope VD, Gallani M, Rowntree PR, Stratton RA (1999) The impact of new physical parametrizations in the Hadley Centre climate model - HadAM3. *Clim Dyn* (accepted)
- Roberts RE, Selby JEA, Biberman LM (1976) Infrared continuum absorption by atmospheric water vapour in the 8 - 12 micron window. *Appl Optics* 15:2085-2090
- Rowell DP, Folland CK, Maskell K, Ward MN (1995) Variability of summer rainfall over Tropical North Africa (1906-92): Observations and modelling. *Q J R Meteorol Soc* 121:669-704
- Sikka DR, Gadgil S (1980) On the maximum cloud zone and the ITCZ over Indian longitudes during southwest monsoons. *Mon Weath Rev* 108:1840-1853

- Slingo A (1989) A GCM parametrization for the shortwave radiative properties of water cloud. *J Atmos Sci* 46:1419-1427
- Slingo A, Wilderspin RC (1986) Development of a revised long-wave radiation scheme for an atmospheric general circulation model. *Q J R Meteorol Soc* 112:371-386
- Slingo JM, Sperber KR, Boyle JS, Ceron J-P, Dix M, Dugas B, Ebisuzaki W, Fyfe J, Gregory D, Gueremy JF, Hack J, Harzallah A, Inness P, Kitoh A, Lau WK-M, McAvaney B, Madden R, Matthews A, Palmer TN, Park C-K, Randall D, Renno N (1996) Intraseasonal oscillations in 15 atmospheric general circulation models: results from an AMIP diagnostic subproject. *Clim Dyn* 12:325-357
- Smith RNB (1993) Experience and developments with layer cloud and boundary layer mixing schemes in the UKMO Unified Model. In: *Proceedings of ECMWF Workshop on the 'Parametrization of the cloud-topped boundary layer', 8-11 June 1993, Shinfield Park, Reading, Berks, UK.*
- Soman MK, Kumar KK (1993) Space-time evolution of meteorological features associated with the onset of Indian summer monsoon. *Mon Weath Rev* 121:1177-1194
- Sperber KR, Hameed S, Potter GL, Boyle JS (1994) Simulation of the northern summer monsoon in the ECMWF model: Sensitivity to horizontal resolution. *Mon Weath Rev* 122:2461-2481
- Sperber KR, Palmer TN (1996) Interannual tropical rainfall variability in general circulation model simulations associated with the Atmospheric Model Intercomparison Project. *J Clim* 9:2727-2750
- Sperber KR, Slingo JM, Annamalai H (1998) The relationship between intraseasonal and interannual variability during the Asian summer monsoon. In: *Proceedings of 23rd Annual Climate Diagnostics and Prediction Workshop, 26-30 October 1998, Miami, Florida.*
- Stephenson DB, Chauvin F, Royer J-F (1998) Simulation of the Asian summer monsoon and its dependence on model horizontal resolution. *J Met Soc Japan* 76:237-265

- Stratton RA (1999) A high resolution AMIP integration using the Hadley Centre model HadAM2b. *Clim Dyn* 15:9-28
- Webster PJ, Yang S (1992) Monsoon and ENSO: Selectively active systems. *Q J R Meteorol Soc* 118:877-926
- Xie P, Arkin PA (1997) Global precipitation: a 17-year monthly analysis based on gauge observations, satellite estimates and numerical model outputs. *Bull Am Meteorol Soc* 78:2539-2558

## Figure Captions

**Figure 1** - Horizontal winds at 850 hPa and 200 hPa for MJJAS, averaged over the AMIP decade. (a and b) HadAM3; (c and d) differences between HadAM3 and HadAM2b; (e and f) ERA.

**Figure 2** - Precipitation (mm/day) for MJJAS, averaged over the AMIP decade. (a) HadAM3; (b) differences between HadAM3 and HadAM2b; (c) CMAP/O.

**Figure 3** - Annual timeseries of monthly mean rainfall averaged over the AMIP decade from the two model runs (solid and dotted lines) compared with CMAP/O (dashed). (a) Indian region (5-30N 70-85E); (b) Bay of Bengal (10-30N 85-100E); (c) East Asian region (5-30N 100-115E).

**Figure 4** - Monsoon onset date calculated using the objective method of Tschuck (see text for details). (a) HadAM2b; (b) HadAM3; (c) ERA (reproduced from Annamalai et al. 1998a). Date is in days from 1st May.

**Figure 5** - Webster-Yang broadscale monsoon intensity index for MJJAS, for each model run and the ECMWF reanalyses. The bars indicate estimates of internal model variability (see text for details).

**Figure 6** - Seasonal mean (MJJAS) precipitation anomalies, averaged over different parts of the monsoon region, for the two model runs and the CMAP/O data. The bars indicate estimates of internal model variability.

- Figure 7** - Precipitation differences (MJJAS) in the equatorial region between El Nino and La Nina years; (a) HadAM3; (b) HadAM2b; (c) CMAP/O.
- Figure 8** - The first two empirical orthogonal functions (EOFs) of precipitation for the two model runs; (a and c) HadAM3; (b and d) HadAM2b.
- Figure 9** - Probability density functions (PDFs) of PC1 from HadAM3 (solid) and HadAM2b (dashed). The dotted line shows the PDF for HadAM3 when only years where the standard deviation of PC1 is greater than 1 are used.
- Figure 10** - Differences in the ten-year MJJAS mean (a and b) horizontal winds at 850 hPa and 200 hPa, and (c) precipitation, resulting only from changing to the Edwards-Slingo radiation scheme.
- Figure 11** - The first two empirical orthogonal functions (EOFs) of precipitation for the run of HadAM3 but with the radiation scheme as in HadAM2b.
- Figure 12** - Difference in the ten-year average onset dates (see text) resulting only from the inclusion of the Met. Office Surface Exchange Scheme (MOSES).
- Figure 13** - Differences in the ten-year MJJAS mean (a and b) horizontal winds at 850 hPa and 200 hPa, and (c) precipitation, resulting only from the inclusion of convective momentum transport.
- Figure 14** - Ensemble average changes in daily mean fields due to inclusion of CMT; (a) change in divergence at 970 hPa; (b) change in increment to divergence by convection scheme at 970 hPa; (c) change in increment to divergence by boundary layer and convection schemes at 970 hPa; (d) change in divergence at 200 hPa; (e) change in increment to divergence by boundary layer and convection schemes at 200 hPa; (f) change in precipitation.
- Figure 15** - Difference in the ten-year average onset dates (see text) resulting from the inclusion of CMT.
- Figure 16** - Differences in the ten-year MJJAS mean (a and b) horizontal winds at 850 hPa and 200 hPa, and (c) precipitation, resulting only from the removal of the rapidly-mixing boundary layer scheme.



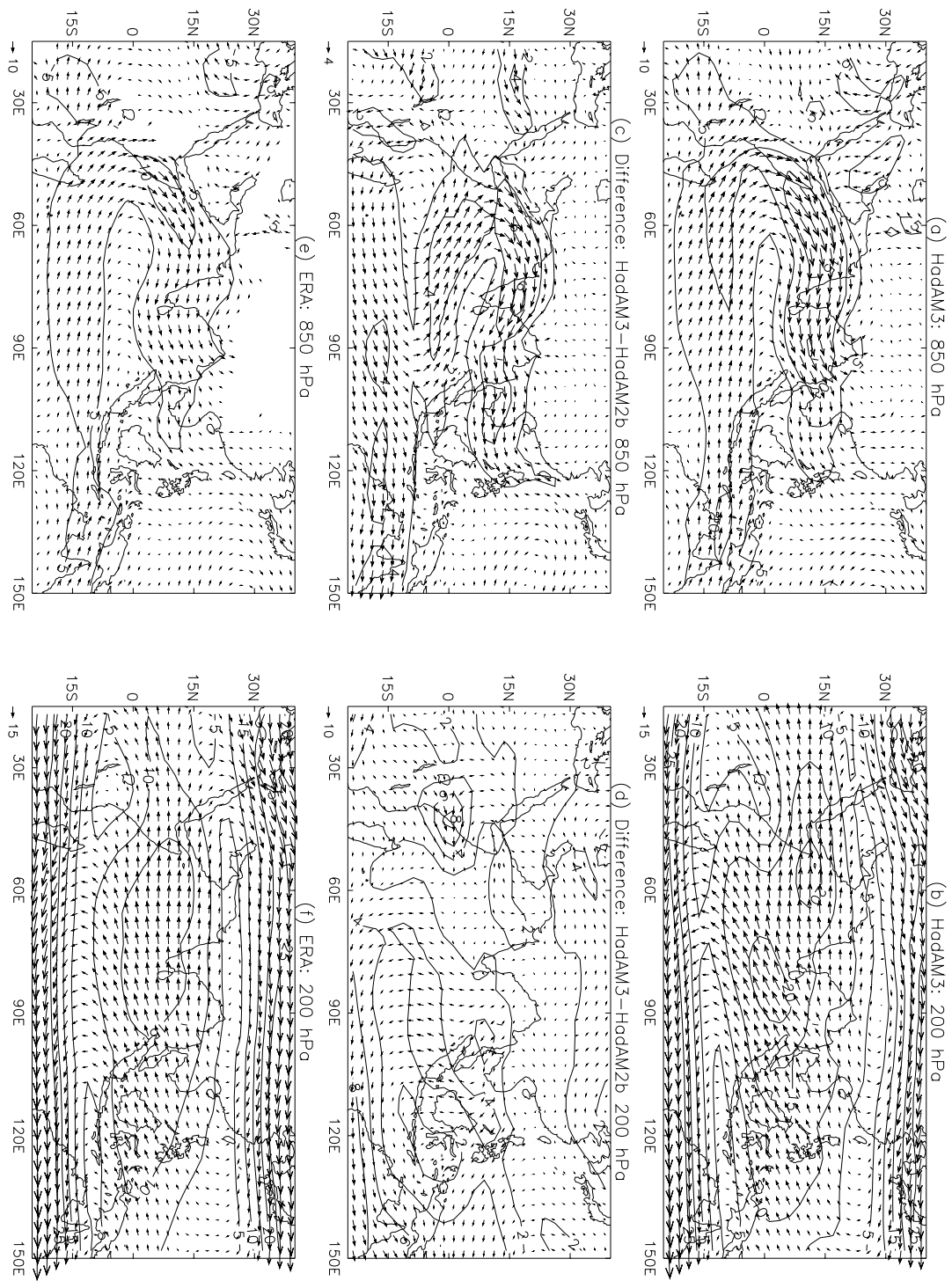


Figure 1:

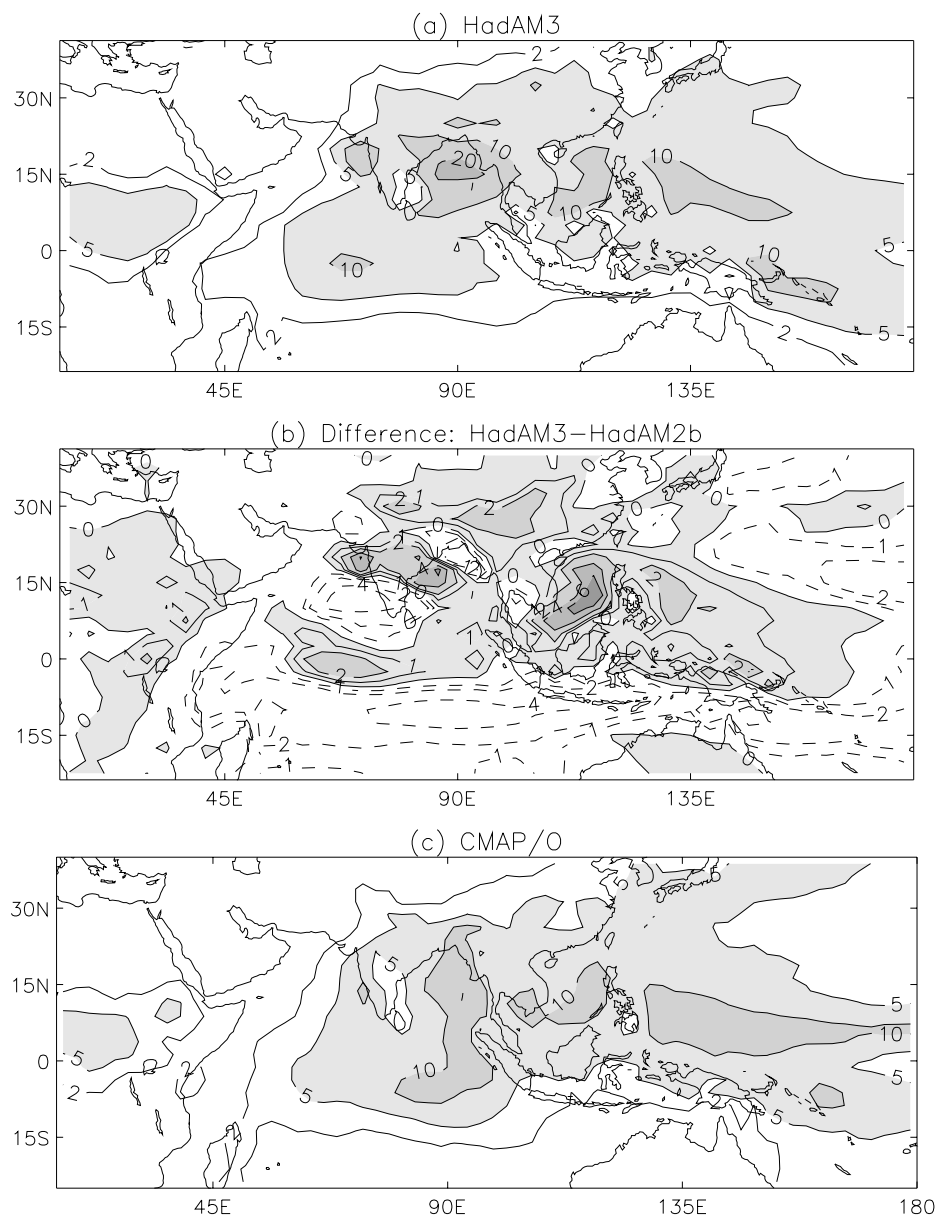


Figure 2:

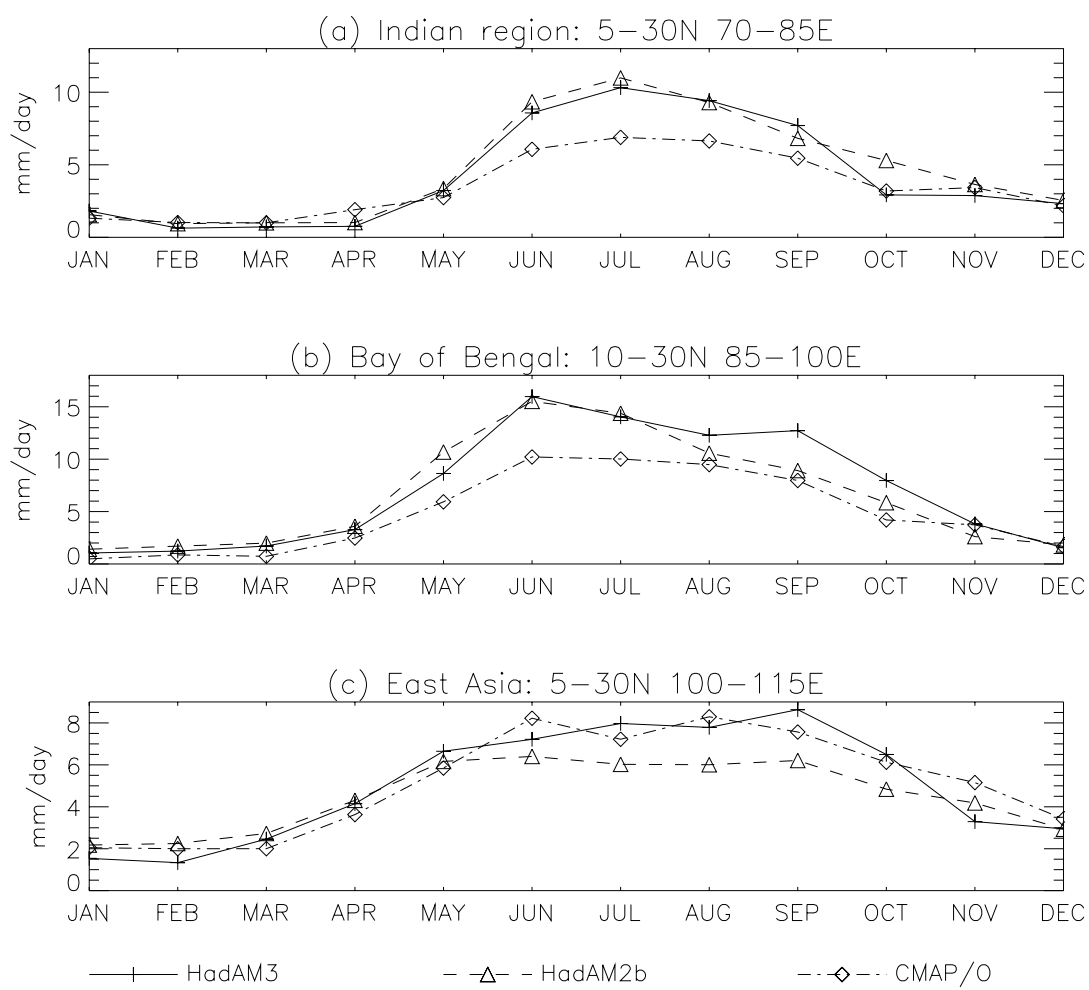


Figure 3:

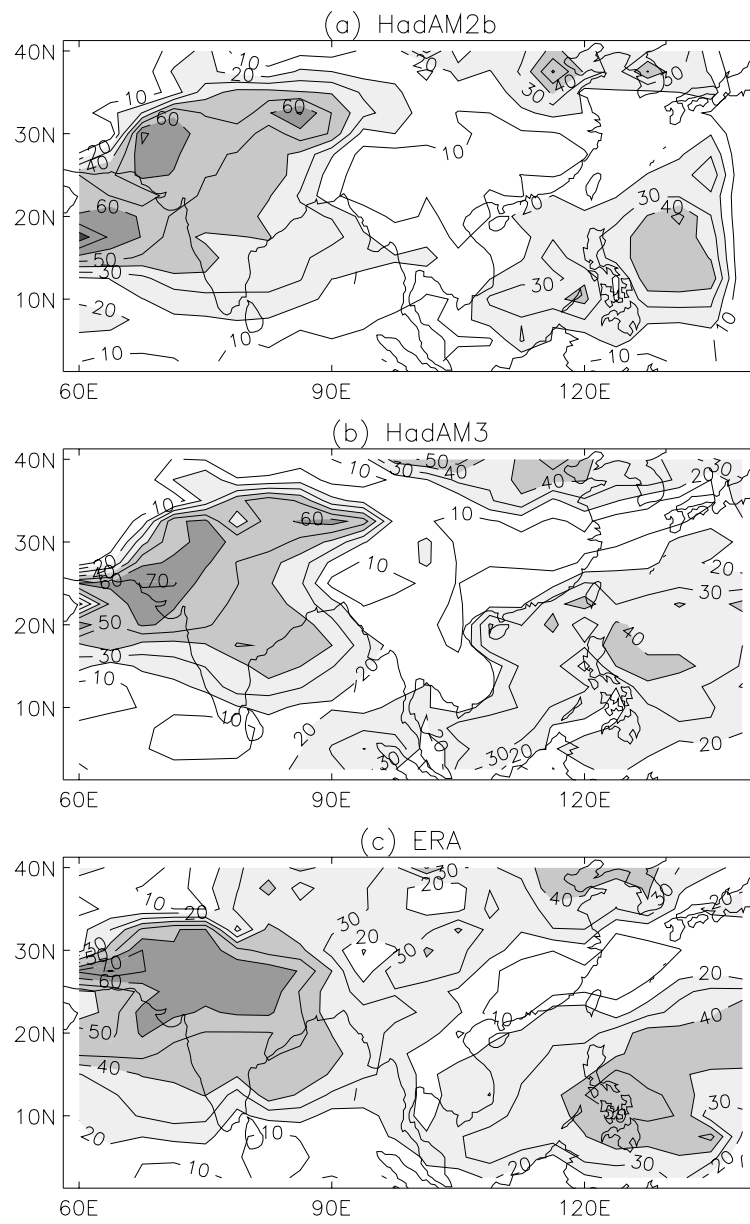


Figure 4:

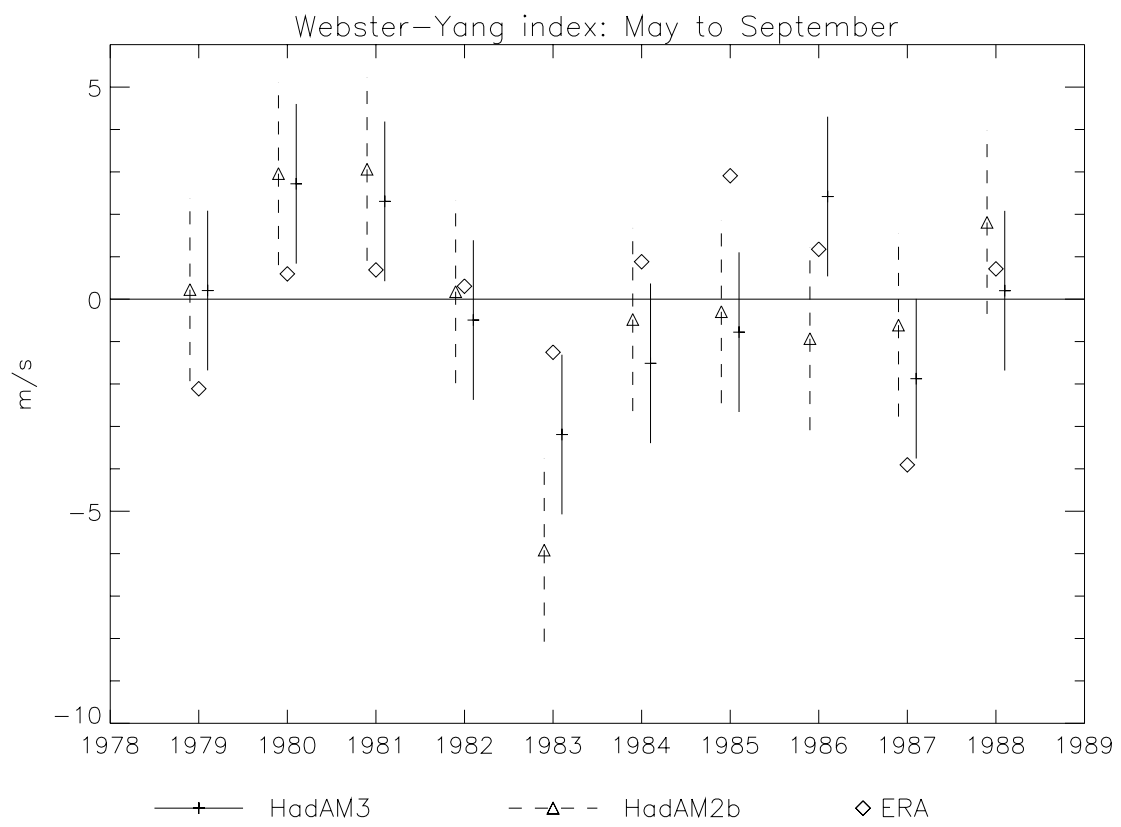


Figure 5:

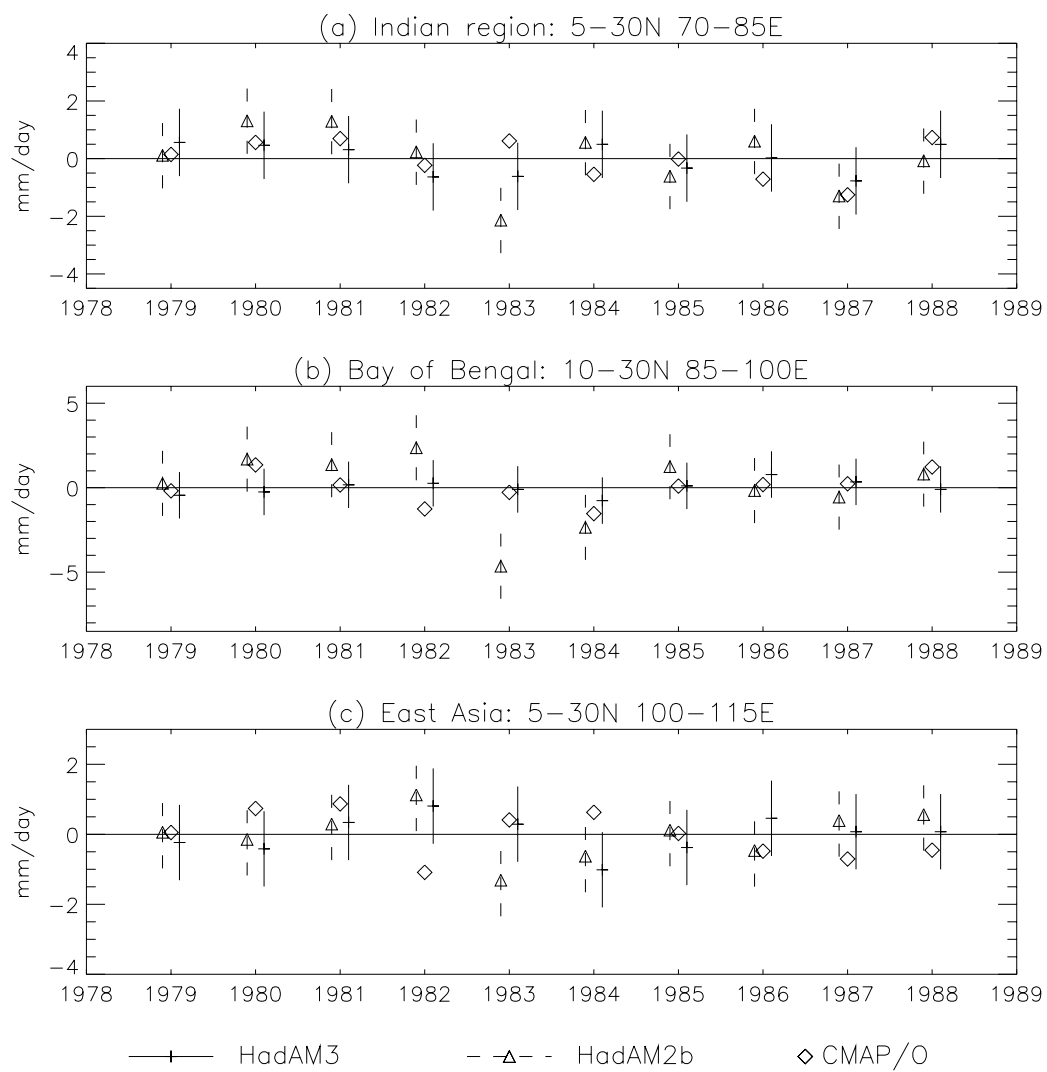


Figure 6:

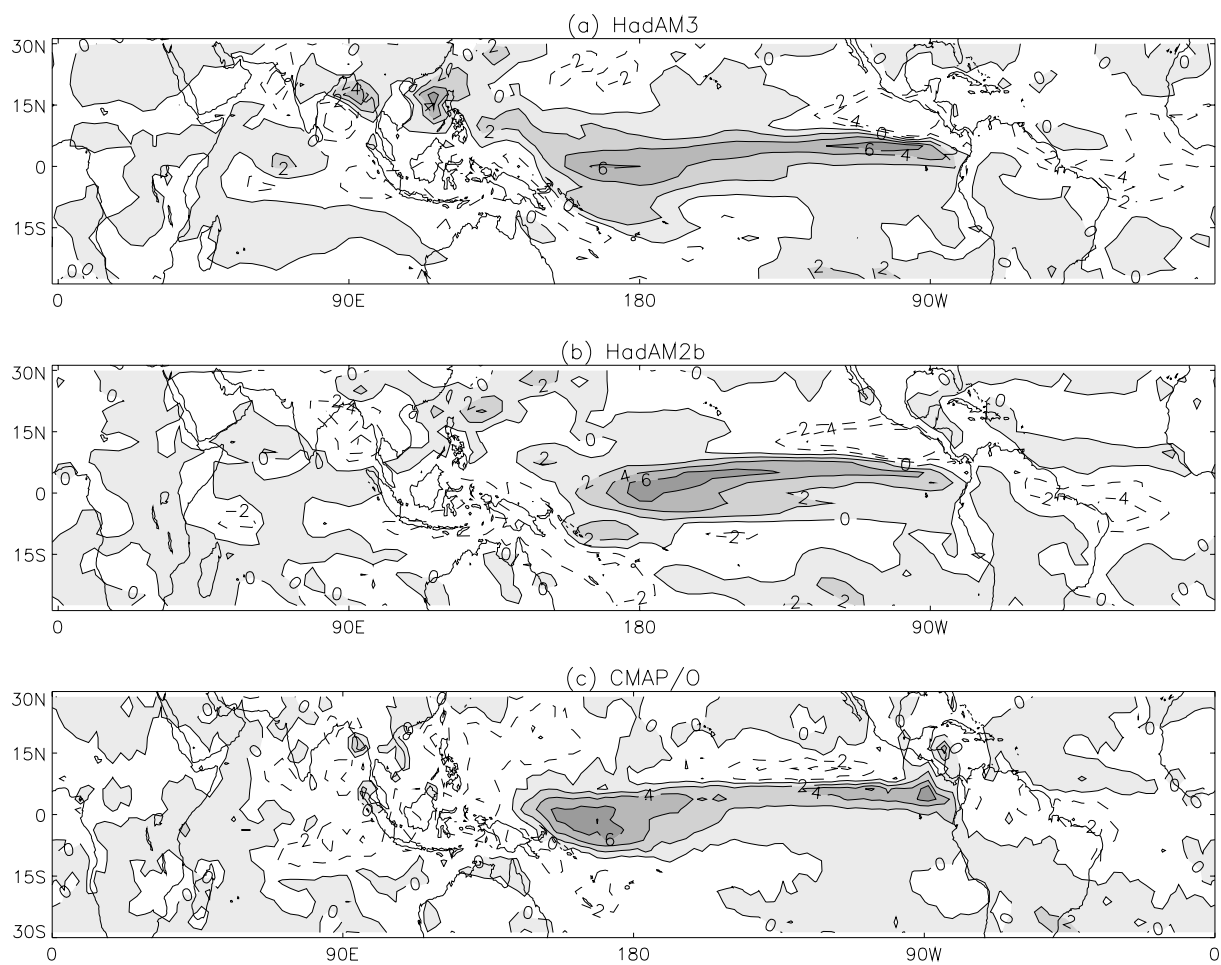


Figure 7:

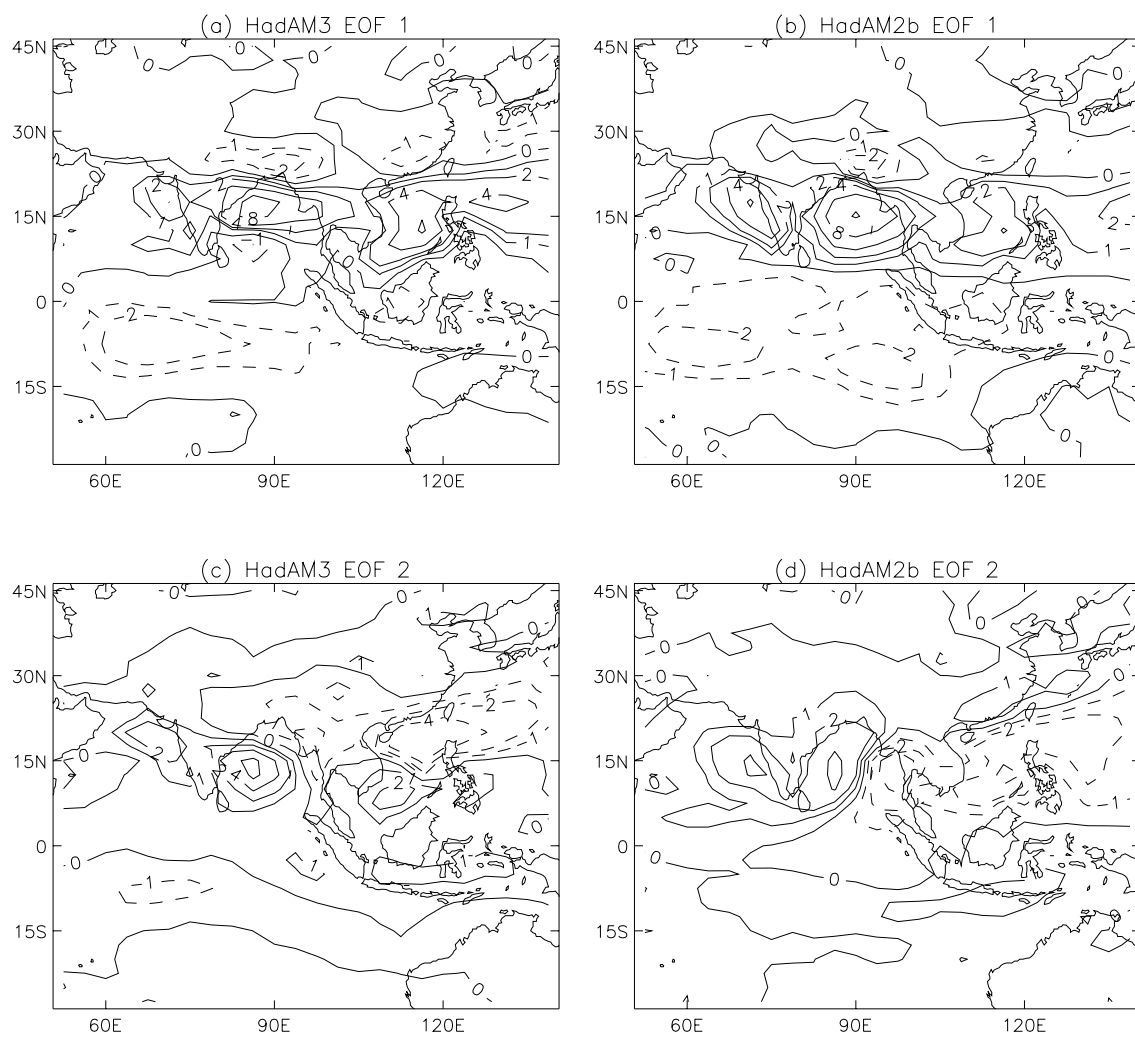


Figure 8:



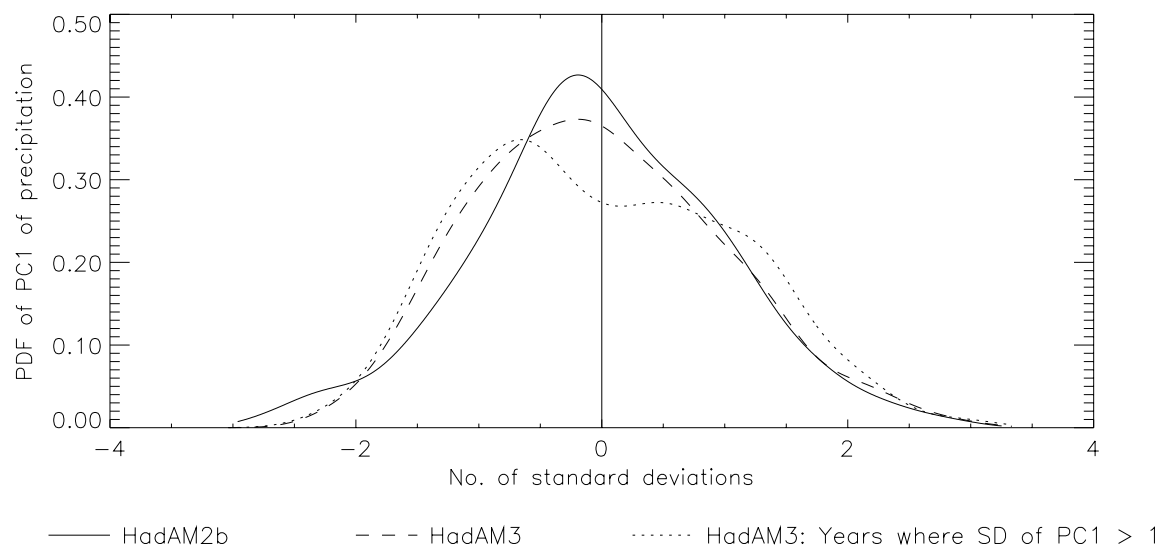


Figure 9:

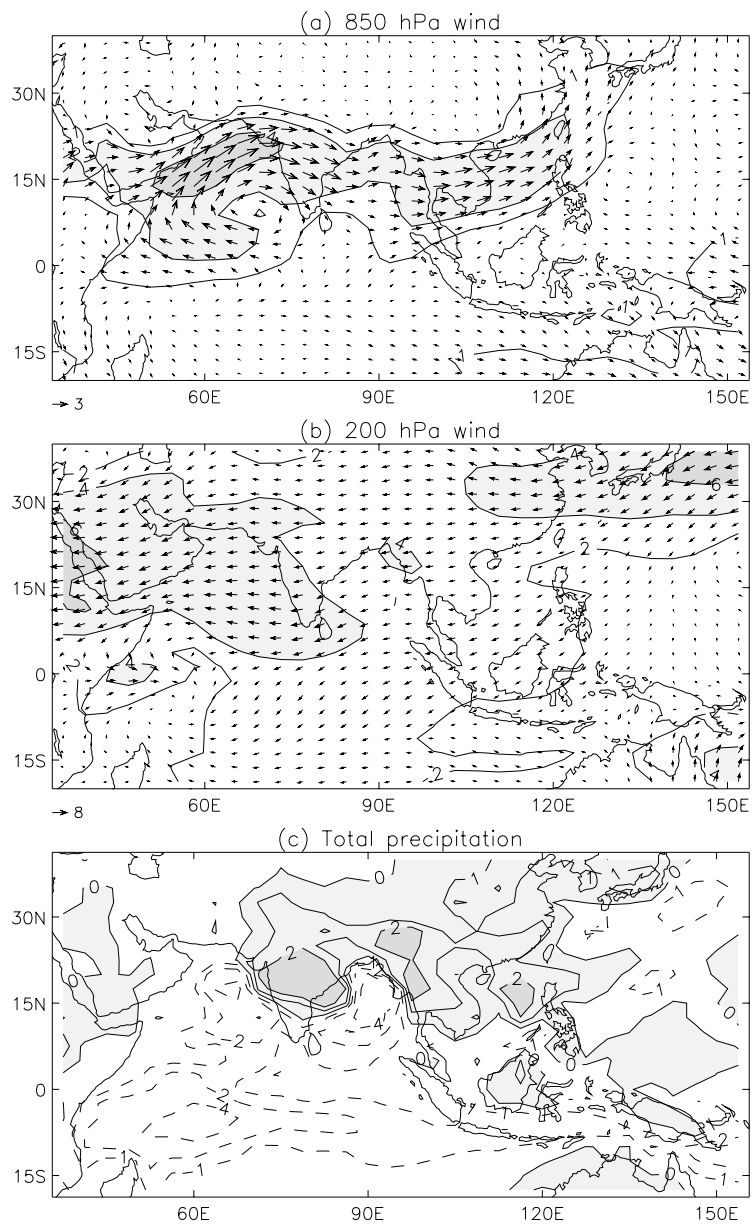


Figure 10:

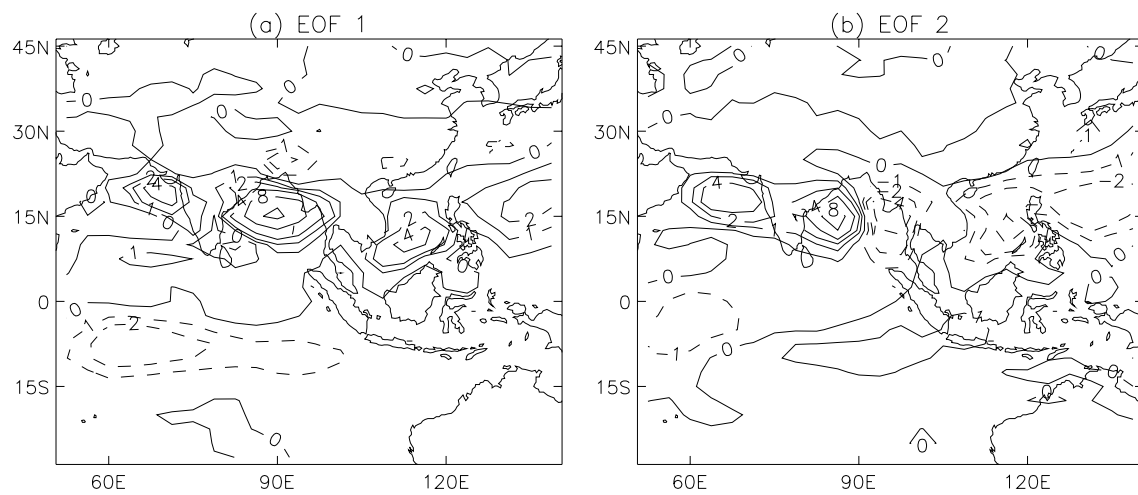


Figure 11:

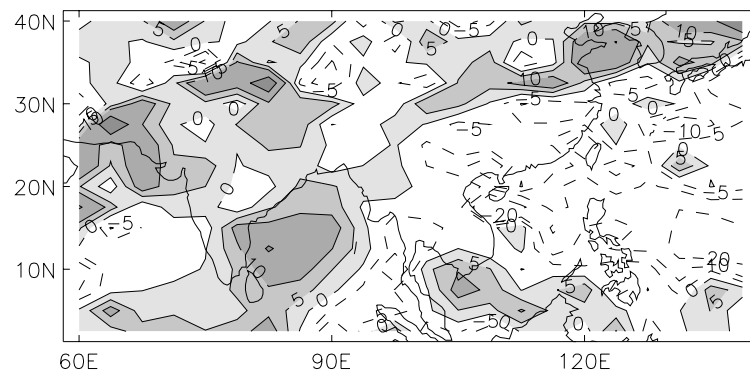


Figure 12:

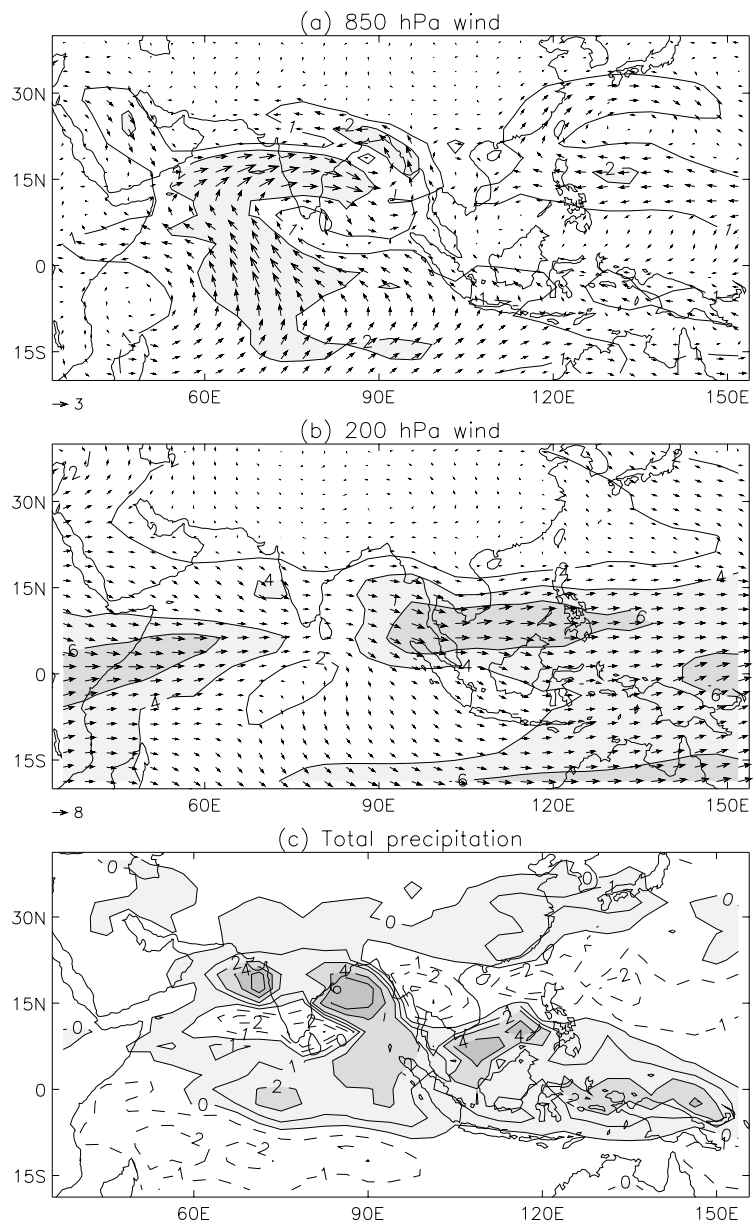


Figure 13:

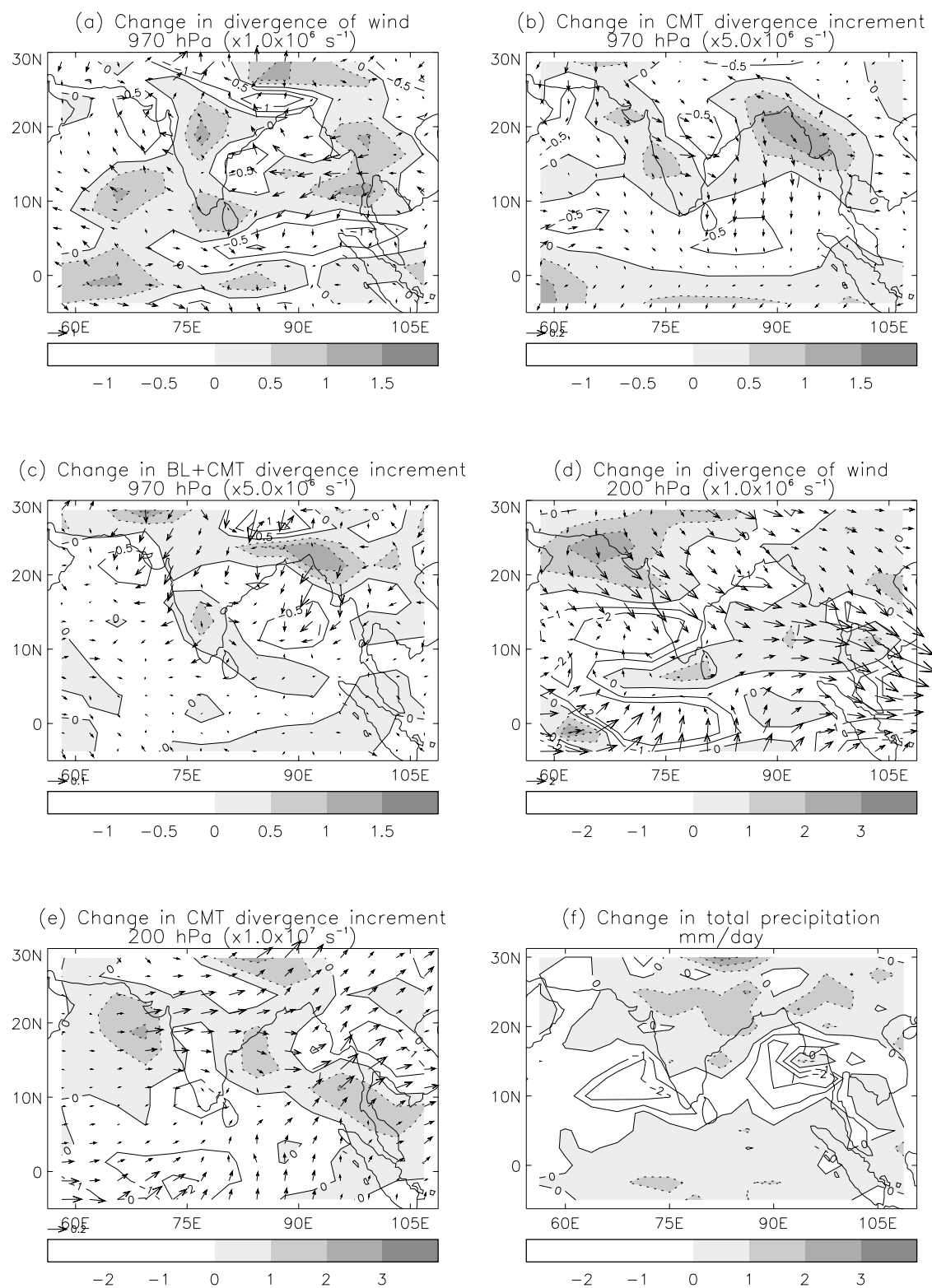


Figure 14:

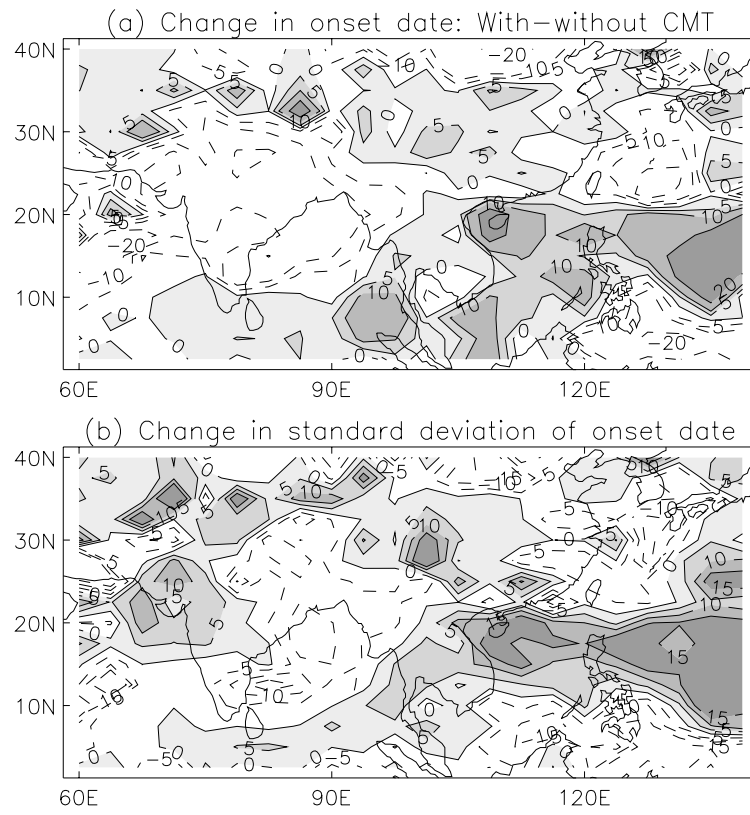


Figure 15:

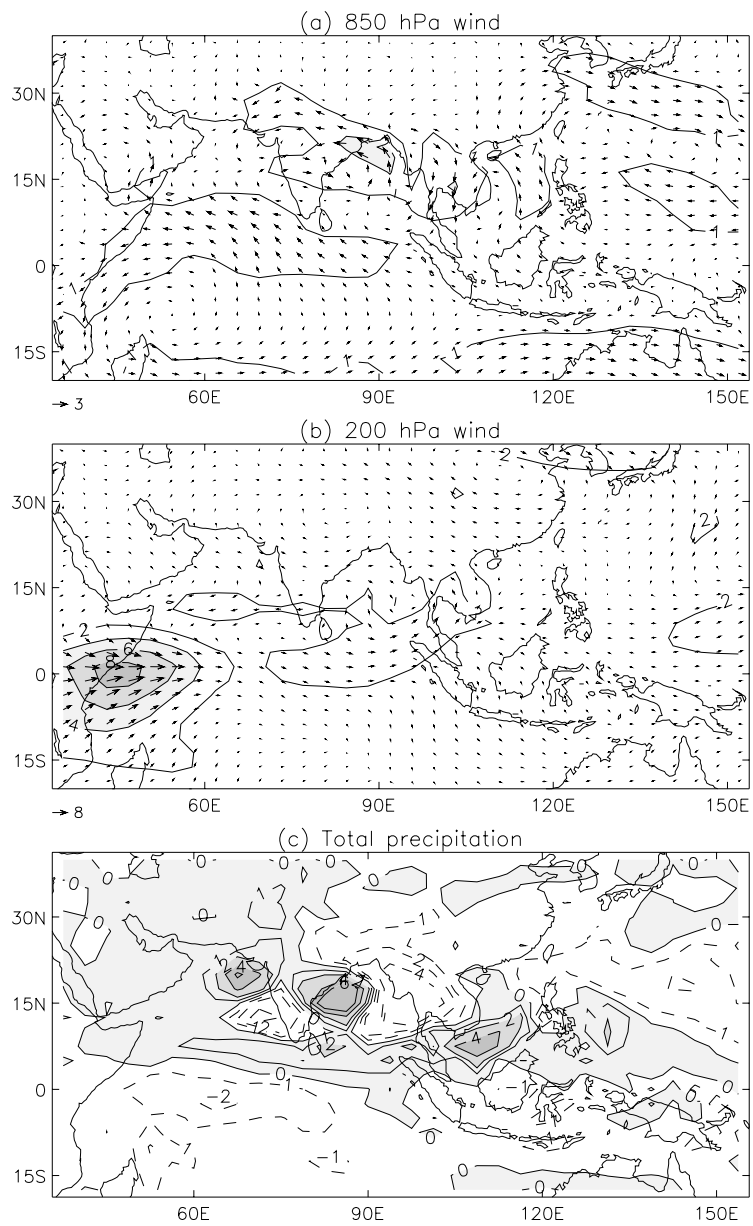


Figure 16: